Title
Electronic Differentials for High-Performance Electric Racecars

Author
Nguyen Huu, Patrick

Publication Date
2014

Peer reviewed|Thesis/dissertation

UNIVERSITY OF CALIFORNIA,
IRVINE

Electronic Differentials for High-Performance Electric Racecars

DISSERTATION

submitted in partial satisfaction of the requirements
for the degree of

DOCTOR OF PHILOSOPHY

in Mechanical and Aerospace Engineering

By

Patrick Nguyen Huu

Dissertation Committee:
Professor J. Michael McCarthy, Chair
Professor Roger McWilliams
Professor Timothy Rupert

2014

DEDICATION

To

my family and friends.

For standing by me in support and aid,

and weathering the storm.

Without whom I would be lost,

adrift in the sea of life.

If hope is the engine of the soul,

then duty is the nagivator...

and love is the fuel.

- Sani Rifati

Table of Contents

Page

List of Figures

Page

List of Tables

Page

ACKNOWLEDGEMENTS

I would like to express the deepest appreciation to my committee chair, Professor J. Michael McCarthy, who has picked me up and guided me through the last several years of work, and has always been convinced of the future success of all of his students. Without his guidance and persistent help, this dissertation would not have been possible.

I would also like to thank my committee members, Professor Roger McWilliams and Tim Rupert, whose advice and input have been instrumental in guiding my work and focusing the research.

In addition, a thank you to Professor Robert Liebeck, who has been a steady source of support and guidance for many years, and whose enthusiasm and engagement for this work were sorely missed during my defense.

And a thank you as well to Robert Smith, whom we all call Smitty, who has been absolutely vital to the success of my research with his advice and knowledge of, well, just about everything.

Finally, the largest debt is owed to my family and friends. My family, who during these years have supported me unconditionally, whom I have sometimes argued with and who, despite this our difference of opinion at times, have allowed me to walk my own path. To my mother and father, whose tireless work allowed me this opportunity, and the rest of my family, who have always been there: thank you. To my aunts and uncles, who always had words of encouragement for me: thank you. To my grandmother, whose silent encouragement and wonderful smile gave me the will to press on, and my grandfather, who couldn't see me graduate: I hope I've made you proud.

And my friends, who have also supported me, and have helped me grow, who saw something worth nurturing and befriending. Friends without whom I would not be the person I am today, and who have helped shaped my perception of the world. Thank you, Jay and Del, Sheila and Shari, because without you, I wouldn't be who I am now.

My friends and colleagues, without whom this thesis would not be complete, and without whom I would not be here, to Epsilon team! Peter, Kevin, Devin, Ray, this one's for you.

CURRICULUM VITAE

Patrick Nguyen Huu

2008	B.S. in Mechanical Engineering, University of California, Irvine B.S. in Aerospace Engineering, University of California, Irvine
2008-10	Research Assistant, Department of Aeronautics and Astronautics, Purdue University
2010	M.S. Aeronautical & Astronautics Engineering, Purdue University
2011	Teaching Assistant, Mechanical & Aerospace Engineering, University of California, Irvine
2011-14	Research Assistant, Mechanical & Aerospace Engineering University of California, Irvine
2014	Ph.D. in Mechanical & Aerospace Engineering, University of California, Irvine

FIELD OF STUDY

Electric powertrains for performance vehicles.

PUBLICATIONS

P. Nguyen Huu and J. M. McCarthy, "Design of an Electronic Differential for a Formula Electric Racecar," *Proceedings of the IEEE International Electric Machines and Drives Conference,* pp 62-66, May 12-15, 2013, Chicago, Illinois, USA.

P. Nguyen Huu and J. M. McCarthy, "Design Considerations for the High-performance Power-efficient Electric Racecar," *Proceedings of the IEEE Vehicle Power and Propulsion Conference,* pp. 1194-1197, October 9-12, 2012, Seoul, South Korea.

P. Nguyen Huu, S. Luu, M. Garcia, K. Chang, and L. Zaragoza, "Plasma-Assisted High Lift Systems," *Proceedings of AIAA 27th Applied Aerodynamics Conference,* paper no. 2009-3943, June 22-25, 2009, San Antonio, Texas.

ABSTRACT OF THE DISSERTATION

Electronic Differentials for High-Performance Electric Racecars

By

Patrick Nguyen Huu

Doctor of Philosophy in Mechanical & Aerospace Engineering

University of California, Irvine, 2014

Professor J. Michael McCarthy, Chair

The use of electric motors in automotive performance applications has resulted in the development of the electronic differential, and the capabilities stemming from independently-controlled wheels. The potential benefits have been explored before; however, there is little experimental data published on the effects of such a vectored torque system on the performance of an automobile. This thesis will investigate the effects of such a system on a rear-wheel driven Formula-Student class racecar with regards to its performance on the skid pad and track.

Experimental data is collected from the skid pad as well as a modified figure-four course and compared to a calculated estimate to find the optimal torque bias for a given vehicle and driver to maximize cornering speed and stability. In doing so, skid pad and course times were acquired for two test vehicles with a variety of static torque bias settings which were then further implemented on a course. The resulting data indicates that the vectored torque system increases vehicle performance regardless of the driver and aids in controllability of the vehicle.

Nomenclature

v	Velocity
t_r	Vehicle track (center-to-center wheel distance for the front or back tyres across the width)
r	Turn radius
δ	Ackerman steering angle
α_f, α_r	Front and rear slip angle
α	Steering angle
$d_{suspension}$	Suspension displacement

1. Introduction

1.1 Research Goal

The goal of the research pursued in this dissertation is the testing, evaluation, and documentation of a directed torque-controlled system for traction control and stability improvements in a racing application, specifically, under lateral accelerations exceeding 1g. In order to accomplish this goal, two different vehicles were tested as a platform for a torque vectoring system and the resulting performance compared over a baseline measurement. Applied metrics were their performance for a number of different drivers with different driving preferences and experiences on both the skidpad with regards to time and stability, as well as a custom track.

Though there is currently little data on the actual effects of a torque control system for automotive applications published, the potential uses are numerous, with several theoretical and experimental attempts investigating applications in suspension control, independent motive power, as well as traction control. However, of those, only a few have focused on the experimental quantification of a torque-vectored tractive system for automotive applications, and as such, the goal of this research thesis is the design and assessment of a prototype torque-vectoring system for a rear-wheel drive vehicle and its effects on the vehicle's performance, as well as an investigation into the potential variables that could affect the change in performance from vehicle to vehicle, under racing conditions such as in Formula SAE.

1.2 Literature Review

The emergence of electric motors and their use within road vehicles has caused a development shift away from the traditional single-engine, single-driveshaft automotive setups, and enabled the design of more varied drivetrains. While there are still single-engine electric drives, multi-motor electric vehicles have allowed the implementation of independent drive systems for road vehicles in which each wheel may be actively or passively controlled by the onboard system depending on the situation. The advantages of such a system are still being explored, but it opens the gate for concepts such as torque-vectoring.

The road equivalent of vectored thrust in aircraft, a torque vectoring road vehicle uses an electronic rather than mechanical differential in order to split the torque output of its motor or motors to the wheels. Where a conventional, internal-combustion engine powered car would connect to the powered wheels via a driveshaft, transmission, and mechanical differential - something that is still possible for single-motor electric drive systems - independently driven wheels have allowed the deployment of truly independently adjustable torque and power levels to the driven wheels.

Electric motors, which, unlike their internal combustion engine counterparts, develop maximum torque at zero rpm, have necessitated the development of more complex electronic differentials in order to take advantage of the benefits they have over internal combustion engines, allowing for greater flexibility in how the power-to-wheel is transmitted and adjusted depending on the driving condition. This allows for real-time adjustment beyond the static rpm-based difference that is caused by mechanical differentials. In an electric vehicle, four- or even just two-wheel drive is capable of independently controlling motor output from the shaft to the wheel, contributing to stability, steering assist, and improving handling.

The most basic approach to electronic differentials is a straight rpm differential between the two driven wheels based on steering angle, similar to a mechanical differential. Further additions to this basic electronic differentials have been proposed and made over time in order to have the motors and control system adjust to different situations according to different inputs, such as digitally controlled direct-torque control (DTC) applications [1]-[4]. Wang et al. [5] apply this with regards to assisted steering wherein the control system takes into account the required torque differential between the inside and outside wheels at any given steering angle in order to supplement power steering. Conversely, there is also the possibility for such a system to actively alter the way a vehicle handles on the road, that is, to deliberately alter and tune the driving characteristics of a vehicle, potentially to better match a driver or the course by changing the torque differential between the inside and outside wheels.

Besselink [6] has proposed a similar system wherein steering and traction are integrated utilizing the differential driving torque of the rear axle to assist steering; such a system would allow the tractive system to actively detect suspension displacement and calculate contact patch area, then adjust wheel torque for optimal grip on uneven surfaces. A different form of vectored torque is suggested by Jang et al. [7] through the use of differential braking in order to correct steering maneuvers by matching the applied wheel torque at the ground to the traction limit of the steering maneuver. In the same vein, Wang et al [5] builds on the potential of such systems to present a computerized torque control system for 4WD vehicles to supplement power steering by actively monitoring and controlling the applied torque to the wheels to prevent slippage.

In most cases, a DTC-based electronic differential is used due to its simplicity, as it does not require rpm sensors, voltage, or current measurements, or position encoders, and has a faster dynamic response time due to the lack of a proportional-integral current controller [8]-[10].

However, they have issues providing similar performance benefits at low speeds, and much work has gone into improving circuitry and control programming, mainly through the use of adaptive observers for speed and flux estimation [11]-[13].

Nozaki [14] considers the use of a steering-induced torque bias on the rear wheels in order to process steering angle velocity and body slip angle to improve drift running performance, while Perez-Pinal et al. [1] have looked at using differential torque from a stability point of view with regards to the evolving complexity and unreliability of modern electronic differentials and presents a simplified system.

The common factor in all of these is the use of differential torque and the concept of altering a vehicle's stability and driving characteristics through the application of torque, whether by direct torque control, or torque limitations such as braking. Tabbache et al [2] follows in the same vein as Perez-Pinal [1] as far as to present a simpler torque control system in order to improve vehicle stability on a two-motor, front wheel-drive vehicle for commercial use in order to increase reliability.

Merkt [15], however, is one of the few to look at the effects of differential torque on vehicles from a purely performance point of view in terms of a racing application. As such, Merkt considers the ability to affect and improve turning behavior and skid pad lap times for a Formula-Student class vehicle. In doing so, he considers the steering angle of the vehicle as the primary input and uses derivations based on Milliken's [16] information to calculate the differential between inside and outside wheel velocity for a given turn radius, shown in eqns 1 and 2:

$$\frac{v_{inside}}{v_{outside}} = \frac{r-0.5t_r}{r+0.5t_r} \tag{1}$$

$$\delta = l/r + (\alpha_r - \alpha_f) \quad (2)$$

where v_{inside} and $v_{outside}$ are the inside and outside wheel velocities, respectively, r is the turn radius, t_r is the track of the vehicle, and l is the wheelbase. Eqn. 2 calculates the required steering wheel angle, while α_f and α_r are the front and rear tyre slip angles, respectively. However, Merkt does not further elaborate on the effects or details of such a differential on the performance of the vehicle on the skid pad.

1.3 Overview of Contributions

This paper will investigate the application of a custom vectored torque system (VTS) on a pair of rear-wheel drive cars in the Formula Student SAE category, and attempt to quantify the extent of the system's effects based on a number of variables, including the driver, road surface, as well as the vehicle itself. The vectored torque system used in this paper is adjustable, and has been tuned for optimal performance on the vehicle and will demonstrate that it is possible and, in some cases, desirable to alter a vehicle's driving characteristics.

The adjustable torque control itself is also being used to develop a theoretical model to predict the optimal setting for a given vehicle based on its basic characteristics, such as weight, track, wheelbase, and the height of its center of mass. This thesis presents experimental results for a VTS system on two vehicles under three different track conditions for novice, experienced, and exceptional drivers. The data shows that on both vehicles, with different driving characteristics, the VTS benefits performance independent of the driver.

Additionally, the results indicate that vehicle driving characteristics can be affected by the VTS through mitigating oversteer and understeer. The results for both vehicles will be compared to one another, and the possibility of further extending the potential results on other vehicles explored.

1.4 Summary

There are numerous papers and experiments based on the use of differential torque for road vehicles; however, very few of them have managed to publish the resulting data, and much of the ongoing research is likely confidential due to the highly competitive nature of the automotive market. Many papers focus on the controls and stability aspect allowed by an independent torque-control system and the impacts of such a controls system for the commercial vehicle market.

However, this research thesis will look at a basic torque-vectoring system in order to provide a quantitative verification of the effects of such a system with a specific focus on traction control and vehicle stability from a powertrain point of view. Besselink [6] has proposed a similar insight, however, instead of looking at the vehicle's driving characteristics on uneven terrain, this thesis will focus on the effects of a torque-vectored drivetrain under high-stress conditions, such as high-speed turns, drifts, and tyre slippage. Merkt [15] has done conceptual work on such a system using purely the steering angle as the input for the torque bias; however, vehicle speed in a turn is also a factor and will be accounted for by the vectored torque system used in this research.

The VTS operates on the basic principle of matching the applied wheel torque to the traction limit of the wheel. Any amount of applied torque over the traction limit causes side-slip and potential loss of control [16]; as such, the main factors contributing to the torque and traction limits of a given vehicle are its base characteristics, that is, its chassis dimensions, weight, front-to-back weight ratio, and available power and torque. By taking these basic parameters into account, a torque-vectoring system is created and tested in order to investigate the benefits on multiple test platforms.

2. Racecar Vehicle Dynamics

2.1 Introduction

A road vehicle undergoing a turn experiences a number of different forces that impact its driving dynamics, handling, and stability. From the front-to-back weight shift that occurs as the driver accelerates or brakes during the turn, to the centripetal force acting on the vehicle's center of mass and causing a body roll, the effect on the tyre contact patch changes the driving behavior, sometimes excessively to the point where control over the vehicle is no longer possible [16]. The vectored torque system presented and examined in this thesis will be used to mitigate one of the main factors that occur during a high-speed turn: tyre slip due to over-torque.

2.2 Vehicle Cornering Dynamics

A vehicle turning a corner experiences a number of forces that can affect its handling adversely. Slippage of the tyres induced by the relative motion of the inside to outside tyres, as well as the forced slowing of the inside tyre due to drag both contribute to wear on the tyres and can cause loss of traction, or catastrophic failure of the tyre. The mechanical differential that has to cope with these forces has undergone a number of iterations, ranging from locked axles to open differentials, each with their respective advantages and disadvantages, which has spurred on the development of the limited-slip differential that is more commonly used today.

Fig.1 shows an extreme example of what can occur during a high speed turn to a vehicle. Under the lateral acceleration, the weight has transferred from the inside to the outside of the car with respect to the turn and, in this case, causing a total loss of traction on the rear left tyre.

Figure 1: FWD car on a skid pad.

During such a turn, weight is transferred from the front and back of the car, depending on the driver's acceleration and braking, as well as from side to side, shown in Figs. 2 and 3. This causes not only a change in contact patch as the tyres "roll under," shifting from the treaded part to the edge of the tyre, but also puts a sideways force on the tyre that can cause it to side-slip.

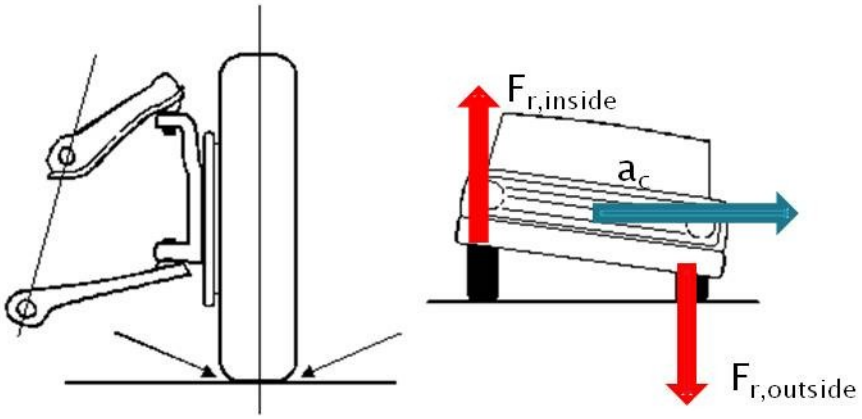

Figure 2: Suspension displacement and forces.

Tyres have a limited amount of "grip," that is, the traction they can provide, which depends on the condition of the tyre, the tread pattern, the condition of the road, and many other factors. All things being equal, however, a tyre subjected to a lateral acceleration is rated for and

can only take so much before losing traction; the specific load and angle a tyre can endure before slipping is provided by the manufacturer under average road conditions, with racing slicks such as the ones used for the following experiments having a higher rated traction and slip angle than road tyres. The maximum available traction to a car is its traction budget, and can be found from both the tyre specifications as well as acceleration runs and comparing the stall torque of the motors to the tyre slip as the vehicle is standing still.

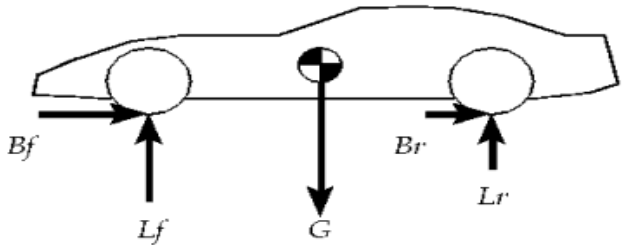

Figure 3: Forces on the tyres.

While moving in a straight line at constant speed under zero acceleration, the traction limit for all tyres solely depends on the front-to-back and left-to-right weight distribution of the car, if tyre conditions and road surface conditions are equal. However, a turn changes these two distributions.

Therefore, in a turn, the maximum lateral acceleration and thus the maximum cornering speed is limited by the traction budget of the car [16]. In a rear-wheel driven car, the cornering traction is lowest on the rear-inside tyre as the weight shifts outside, away from the driven wheel. Based on Merkt's [15] work and Milliken [16], the amount of load the inside tyre can take may then be calculated according to Eqn. 3:

$$F_{r,inside} = a_c \bullet \frac{r_{tire} - d_{suspension}}{t_r} \tag{3}$$

This yields the percentage of traction available to the tyre of the maximum available traction under a given lateral acceleration, and will further be used to estimate starting points for the experimental verification of the torque vectoring system for use on the skid pad, as it considers a constant tangential velocity and therefore no front-to-back weight transfer.

2.3 Electronic Differentials

As a mechanical differential is difficult to use with a multi-motor drive system at best, and many electric vehicles on the road, due to the rpm limitations and wide torque bands of electric motors, do not need a transmission, the counterpart is the electronic differential. With a variable number of inputs, from the basic throttle to the suspension sensors proposed by Besselink [6], the electronic differential interfaces the driver, motor controllers, and motors in order to apply the appropriate amount of torque and rpm given the inputs.

The electronic differential replaces the mechanical differential in a multi-motor electric (or hybrid) vehicle by removing a direct mechanical connection between the powered wheels and electronically controlling and adjusting the drive torque applied to those wheels by the electric motors. As such, it is a purely electronic system that ties into the motor control circuit. By allowing direct and independent control of the driven wheels, the vehicle's driving characteristics can be altered in order to adjust to the problems that would occur - such as an uneven surface, or loss of traction due to slippage. As slippage can occur linearly as well as laterally, torque-matching sensors and controls can be used in order to match the applied torque to the traction limit of a given wheel and tyre, and thus prevent or delay tyre slip in either direction.

In the case of an electronic differential, the calculations to determine torque to apply take place within a computation unit; this can be an external unit interfacing with the motor controllers, or an integral unit within the ECU. In either case, the electronic differential will, on

the most basic level, act to prevent tyre drag and thus wear on the inside tyre during a turn, the same as a mechanical differential. Further capabilities are being explored for numerous applications from ride comfort to 4WD drive control and racing applications.

2.4 Analog Vectored Torque System

The vectored torque system used in this research thesis is a custom-built closed-feedback analog control circuit pictured in Fig. 4 below. The circuit was built and tested in three phases, corresponding with the vehicle performance testing. In order to establish a baseline for comparison, zero vectoring was applied, and the circuit was stripped down to only a single throttle directly feeding into both motors, causing the vehicle to drive as if it had a solid axle. It takes a different approach from the digital DTC electronic differentials used by [1]-[13] by comparing and utilizing the throttle and steering angle inputs directly with a pre-determined torque bias curve.

The VTS is based on a pair of Alltrax AXE7245 motor controllers rated for 450A and 72V, with a 0-5kΩ resistive throttle input. The controllers are programmable and have integrated throttle-up and throttle-down curves. For the purposes of these experiments, a linear throttle-up and throttle-down curve was chosen. The motors and controllers used are current-driven, meaning that the applied torque is directly proportional to the applied current, which is directly regulated by the applied throttle signal. Thus, a given throttle signal will generate a given stall torque for the motor, which allows for precise torque control under side-slip conditions.

The VTS circuit is based on theoretical calculations for the traction limit of the test vehicle, as well as the calculated load shift, which corresponds to the reduced amount of torque that may be applied to a wheel. With the overall signal input required to top out at 5kΩ, as well as maximum throttle being available in a straight line, the circuit was designed to accommodate a

total of 5kΩ resistive output with both the steering and throttle potentiometers maxed out at maximum pedal displacement and zero steering angle, with the steering signal from the inside wheel reducing as the steering angle increases. As it is a two-input system, the resulting output is non-linear, and further discussed in detail in section 4.

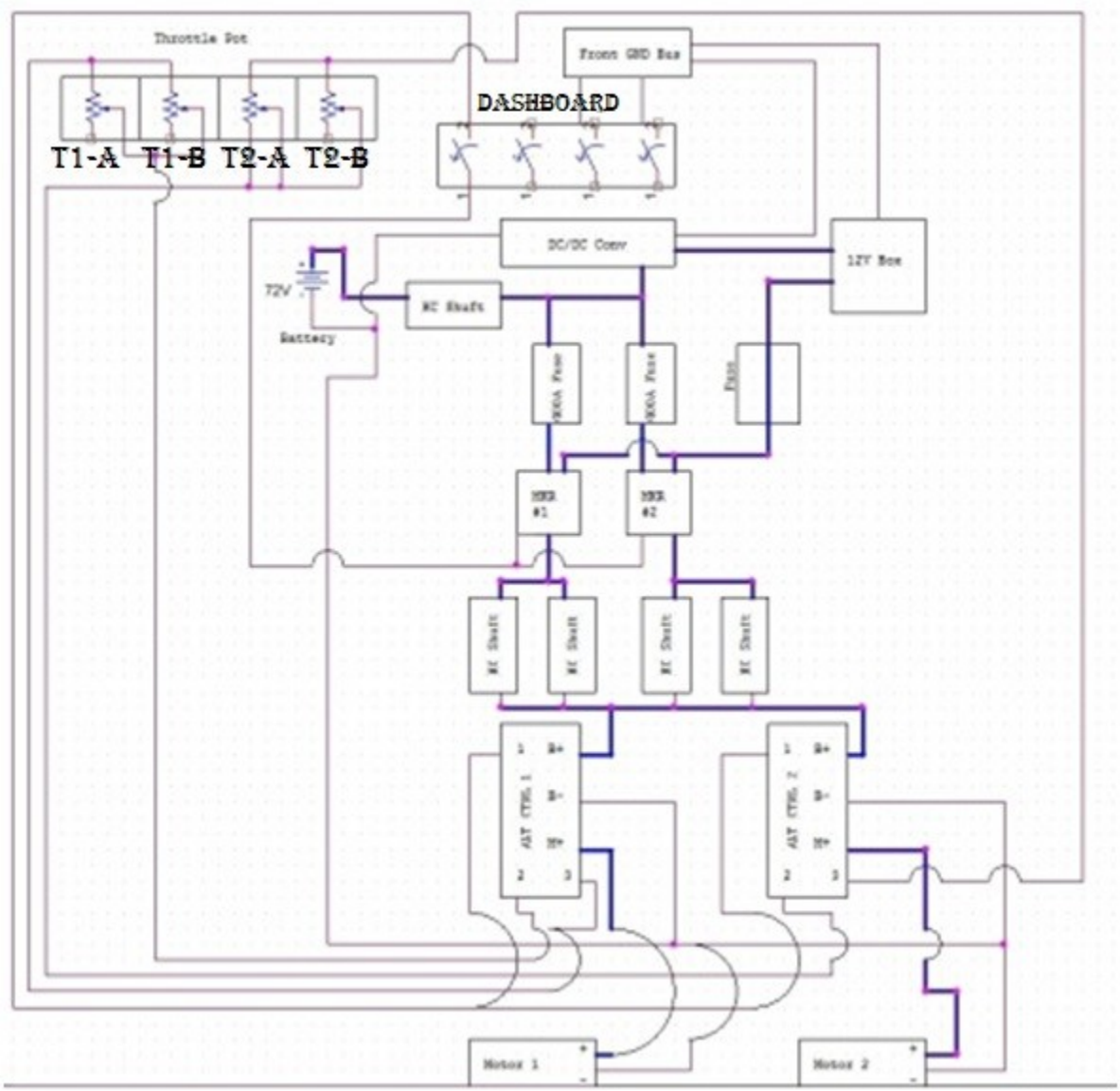

Figure 4-A: Analog torque vectoring circuit.

As shown in Fig. 4, the four potentiometers T1-A, T1-B, T2-A and T2-B denote the four inputs into the circuit for the twin throttle and steering assemblies, respectively. T1-A and T2-A

are the throttle inputs, and fixed at 0-10kΩ potentiometers, with T1-B and T2-B as the steering and offset inputs, respectively, adding up to a total of 0-10kΩ resistance, as well. T1-B and T2-B are then for adjustment purposes further split into an offset and a steering potentiometer, creating the triangular resistance array shown below in Fig. 4-B between the controller input pins 2 and 3:

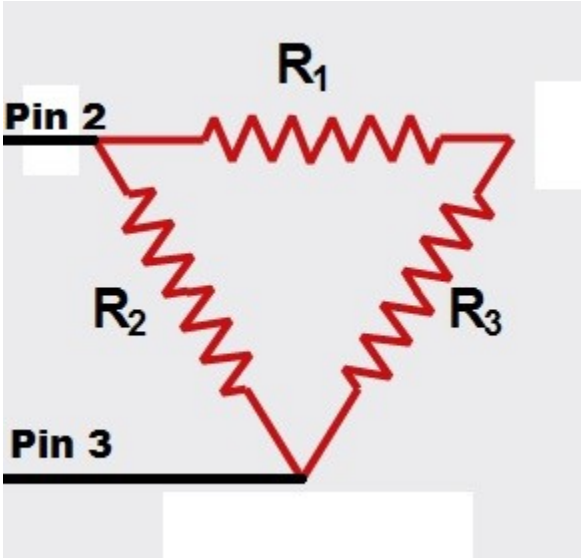

Figure 4-B: Throttle circuit.

In the throttle circuit highlighted in Fig. 4-B, R_1 corresponds to the offset resistance, while R_2 and R_3 are the throttle (T1-A and T2-A) and steering input potentiometers, respectively. By putting the throttle potentiometer (R_2 in Fig. 4-B and T1-A in Fig. 4-A) in parallel with an adjustable offset and the steering input, the maximum of 5kΩ can be achieved when using 10kΩ potentiometers for all three resistors at an offset of zero. With increasing offset, at full throttle, the controller will read a total parallel resistance between pins 2 and 3 of greater than 5kΩ [18]; however, the maximum input signal is capped at 5kΩ, resulting in full throttle.

Further, the circuit was modified to allow for a static setting in which either motor could be independently adjusted to a fixed offset and thus a fixed power ratio between the two. However, it should be noted that it is impossible to increase the outside wheel's torque beyond

full throttle, as the motor controllers do not allow this, and, as such, all testing was conducted on a torque differential of inside-to-outside by dropping the inside wheel's torque. The final and complete circuit comprises a pair of throttle potentiometers connected to a pair of linear sliding potentiometers that are attached directly to the steering linkage and calibrated carefully to a given resistance to steering angle map, along with an offset potentiometer that allows for changing the range of the torque differential based on steering angle and throttle displacement. The offset potentiometers allow for selection of the final, dynamic torque vector range, that is, they are used to dial in the lowest applied torque on the inside wheel under max-load conditions, with a full throttle, maximum steering angle turn.

The static phase of testing was implemented to test and verify the optimal bias setting for a given driver and vehicle and used to calibrate the dynamic offset, which allows the vehicle to adjust the left-to-right torque distribution in real time based on the throttle and steering inputs.

The entire control system is completely analog for simplicity and reliability [1], and consists of a parallel setup of three resistive components, the throttle potentiometer (directly attached to the driver's accelerator pedal), the steering input potentiometer, and a static steering offset resistor that is used to change the range of the torque bias between the wheels for different testing setups, and can later be exchanged for a third dynamic component that can actively alter the torque bias envelope depending on the driving situation. Determining the effect of this adjustment to the throttle input of each motor as well as the optimal level of adjustment depending on the driving situation will then yield a setup that than be further developed for advanced control and stability behavior under a multitude of high-performance conditions. The overall effect has been estimated by assessing the weight transfer as a function of vehicle turn radius to the rear wheels, as well as throttle bias between the inside and outside wheels.

2.5 Summary

In contrast to current digital DTC and flux-oriented [2] control schemes, the vectored torque system proposed in this research is an analog system that operates in a similar manner to a DTC scheme, but takes direct throttle and steering inputs to alter the current output of the controllers to the motors. It takes into account a throttle position encoder as well as a steering angle encoder to determine the speed and turn radius and uses a predetermined algorithm in order to output the appropriate torque differential for the given speed and turn angle.

The analog torque vectoring system used in this thesis is designed to test and allow for the optimization of a calibrated torque-bias system in order to improve vehicle driving characteristics and stability during high-speed turns that put the vehicle under lateral accelerations. It does so by matching the inside wheel's applied torque to the traction limit of that tyre as a function of vehicle speed and turn radius, which were calibrated using skid-pad experiments and then extrapolated for the entire dynamic range of turns and speeds. Offset and input values were based on initial calculations further elaborated in Section 4. Based on Eqn. 3, for a 1g load on the test vehicle, the estimated torque biases for the given skid pad for Gamma and Epsilon were 66% and 55%, respectively; that is, 65% and 55% of the outside wheel's torque applied to the inside wheel under full load conditions.

3. Equipment Design

3.1 Introduction

The experiment uses two different former FSAE cars as the test platforms, each with different characteristics. In order to test the maximum lateral acceleration of these vehicles, as well as their driving performance, they were tested on the skid pad and on a custom track, respectively, while vectored torque system was tweaked and adjusted for data collection. As the primary metric used for the characterization of vehicle performance is the maximum sustainable and controllable lateral acceleration, skid pad times are used to compare the performance of the vehicles with and without the torque control system.

3.2 Overview of Experimental Procedure

All experiments were conducted in order to bracket and optimize the torque bias setting and compare the resulting performance to the baseline with regards to a number of different factors: drivers - and their respective experience - as well as the direction of the turn and the torque bias setting are the primary variables that were adjusted for the experimental process. In addition to that, two very different chassis were used for the experiment in order to compare the effects of the vehicle's dimensions and weight on the effectiveness of the VTS while filtering out human elements and their effects on the test results.

Drivers were separated into three categories for the experiments: novice, experienced, and exceptional. This distinction was made to allow for a measure of comparability between individual drivers and their respective skill levels as well as to evaluate the anecdotal feedback they were able to give from their driving experience in the vehicle during the testing. Novice drivers were classified as those who had zero to little experience in the vehicles and showed the

largest margin of improvement during training. Drivers with a history of driving under racing conditions such as rally drivers or Kart drivers were classified as experienced, and those with little documented history of driving experience and the best skid pad results were classed as exceptional.

Data was acquired by timing the vehicle as it goes around the track, with a few warmup laps given to the driver before the start of data acquisition in order to remove potential hysteresis from the still-acclimating driver. For the purposes of this research, skid pad runs were conducted in sets of six laps each, with two warm-up laps allowing the driver to gain speed and four subsequent timed laps used for data reduction. Additional data on the vehicle's speed as well as its power consumption was acquired via an on-board data logger.

3.3 Testbed 1: Gamma

The first test vehicle used was the 2007-2009 FSAE car called "Gamma," that, in prior incarnations, had been a gasoline, gasoline-electric hybrid, and all-electric vehicle that was converted to a rear-wheel drive electric car with independently powered rear wheels (Fig. 5). As a large vehicle compared to the other former and current FSAE vehicles, it features a large engine bay behind the driver's seat and was chosen for the first conversion to a testbed.

Figure 5: Gamma on the skid pad.

Table 1: PMG-132 specifications.

Voltage	24-72V
Current (continuous/10 min max)	110A / 200A
Weight	24.8lb
Type	DC Brushed
Speed Constant	45 rpm/V
Torque Constant	27 oz-in/A

The main drive train of Gamma consisted of a pair of 7.2kW Perm GmbH PMG-132 permanent-magnet motors powered by a 5kWh LiFePo4 battery pack. Driven at 72V, the PMG-132 performance curve is shown below, in Figs. 6 and 7, with their specifications listed in Table 1. The rear wheels are chain-driven via solid half-axles by the motors, and powered through a pair of Alltrax AXE7245 motor controllers with a 0-5kΩ resistive throttle input.

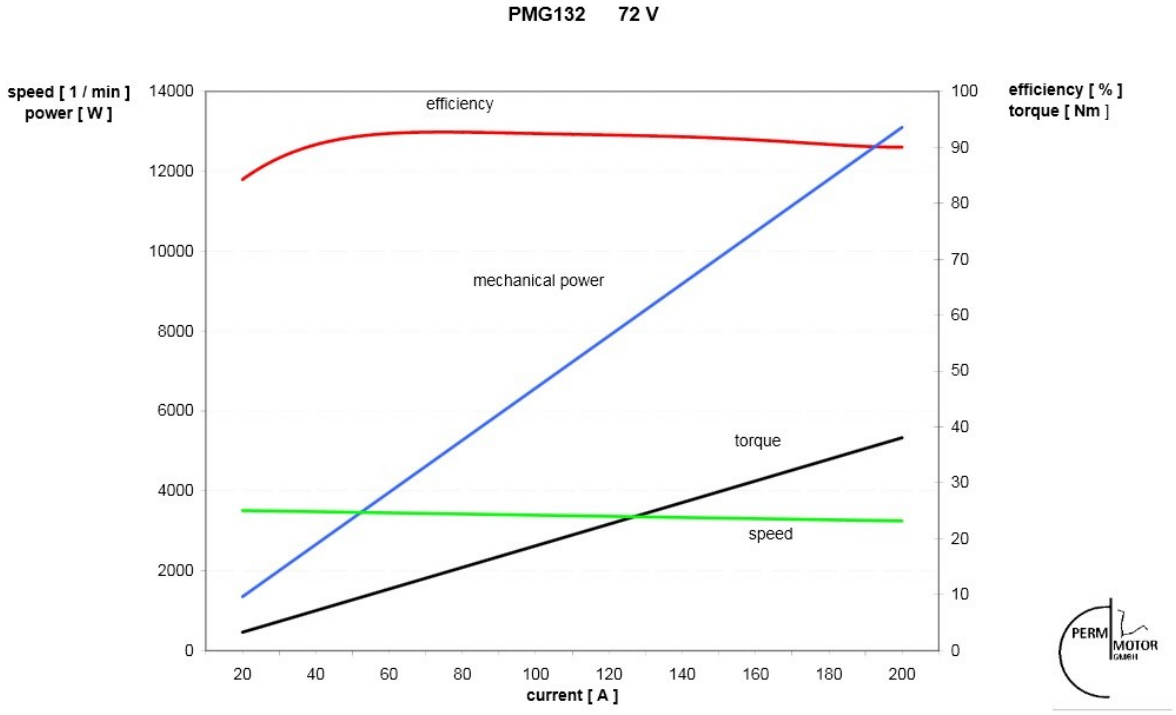

Figure 6: PMG-132 performance characteristics.
(Source: Perm GmbH)

The PMG-132 motors were selected due to their reliability and simplicity; as they put out more than enough torque at the 3.6:1 gear ratio the car was fitted with in order to overcome its static rolling resistance and thus slip the tyres at stall torque. As with most electric motors, the PMGs have a very flat efficiency and torque-speed curve, retaining 75% of their speed over their entire operational current band, allowing for a very direct and simple input current to output torque relationship [19]. Fig.7 is a dynamometer result for the motors run at various voltages and at different load torques conducted under constant speed testing with the braking force increased until the motor stalled at the given rpm, further illustrating the fact that the PMG retains 86% of its rpm at maximum torque, allowing for high linear accelerations of the car at speed [20].

The vehicle was originally tested with the basic throttle setup with a set of 6 12V lead-acid motorcycle batteries with a capacity of 35Ah as a proof of concept before upgrading to the 70Ah LiFePo4 battery pack and the implementation of the VTS.

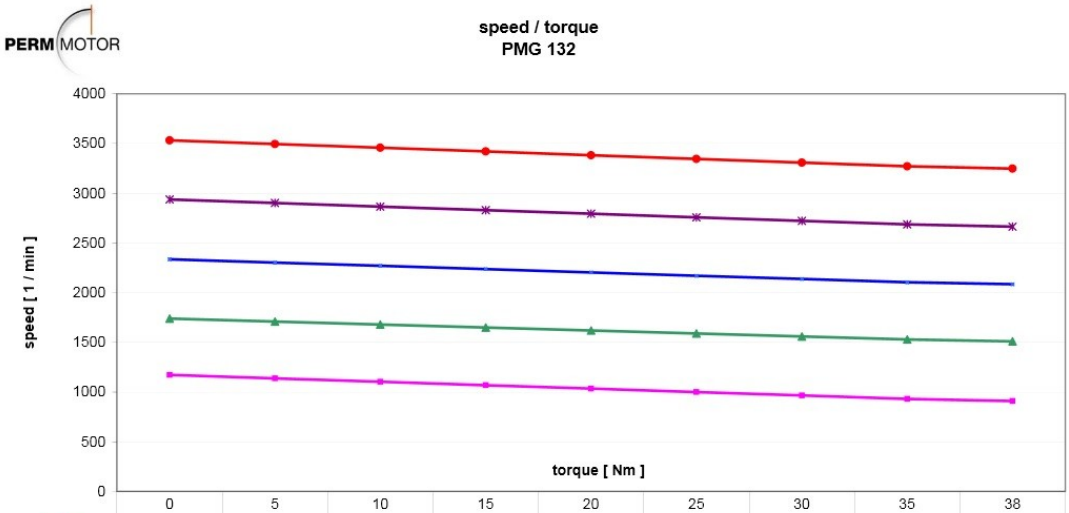

	0	5	10	15	20	25	30	35	38
24V	1172	1138	1103	1069	1034	1000	965	931	910
36 V	1739	1709	1679	1649	1619	1588	1558	1528	1510
48 V	2335	2302	2269	2236	2203	2170	2137	2104	2084
60 V	2937	2901	2865	2830	2794	2758	2722	2686	2664
72 V	3532	3495	3458	3420	3383	3346	3308	3271	3249

Figure 7: PMG-132 speed/torque characteristics. Stall torque measured at a given RPM.
(Source: Perm GmbH)

The specifics of Gamma's chassis are shown below, in Table 2. The chassis was originally constructed to house a motorcycle engine and gas tank directly behind the firewall and as such, the only room for the battery pack was directly behind the driver's seat and low to the ground in order to centralize the mass as much as possible.

Table 2: Gamma chassis characteristics.

Chassis Length	96in
Track	60in
Wheelbase	74in
CG height (unloaded)	2.5in
Weight Distribution (Fore/Aft)	30% / 70%
Weight (without driver)	847.8lb

Despite this, the length of the chassis and the location of the driver's seat, plus the rear-shifted weight of the motors have caused the center of mass to shift rearward, resulting in a 30%-70% front-to-back weight distribution, which has caused severe control issues with the vehicle.

3.4 Testbed 2: Epsilon

The second test vehicle that was used is Epsilon, the former 2011 FSAE car, pictured in Fig. 8 below. With a considerably lighter chassis and a much better weight distribution, this vehicle differs from the Gamma test platform in a number of ways. The wheelbase and track are shorter, and the center of mass is located higher, making for a more compact car.

The chassis characteristics for Epsilon, as well as their comparison to Gamma, are listed in Table 3. The lower weight, along with the smaller chassis made the original, gasoline-powered vehicle much more nimble than Gamma; however, during testing it was discovered that while the PMG motors had enough torque to just slip the tyres on Gamma, the lighter weight and better weight distribution on Epsilon actually lowered its acceleration, as the tyres reached their traction limit earlier.

Figure 8: Testbed Epsilon.

While the shorter chassis also improved the weight distribution, as the engine bay on Epsilon is much more compact, it also necessitated mounting the battery pack higher up, thus raising the center of mass and the roll center of the car. The lighter total weight of the chassis, coupled with the rear-heavy weight distribution resulted in an understeering behavior as opposed to Gamma; this is due to the overall lower weight on the front tyres despite the better weight distribution on Epsilon. The same powertrain, battery pack, gear ratio, controllers, and motors were used on both vehicles, as well as the same VTS circuit. Both vehicles use 13 inch diameter Hoosier racing clicks made from R25B compound in 20x7.5-13 dimensions.

Table 3: Epsilon chassis characteristics.

	Epsilon	**Compared to Gamma**
Chassis Length	80in	-16in
Track	47in	-13in
Wheelbase	63in	-11in
CG height (unloaded)	6.8in	+4.3in
Weight Distribution (Fore/Aft)	38% / 62%	+8% / -8%
Weight (without driver)	692.4lb	-155.4lb

3.5 Track Setup: Skid Pad

The track used for the skid pad testing in order to assess the maximum attainable lateral acceleration of the vehicle is the SAE standard 50ft inside diameter skid pad. The outside diameter was set at 58ft, allowing for an 8ft track vehicle and a nominal track centerline at a radius of 29ft, shown in Fig. 9.

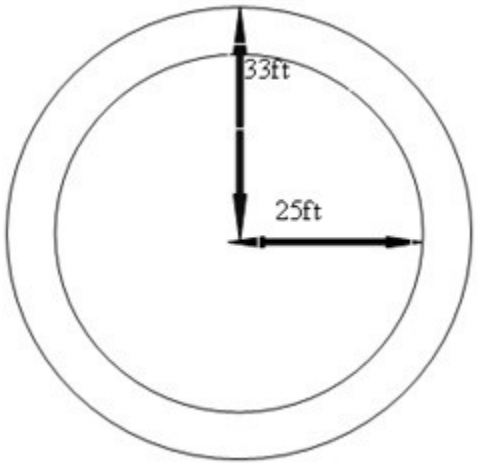

Figure 9: Skid pad setup.

The skid pad surface that was used was the far rear left corner of the 16H parking lot at the University of California, Irvine. This particular surface features a drainage camber around the center post, which induces up to a one degree negative roll in the vehicle. This adversely affected the vehicle's driving characteristics during testing, thus imposing additional stresses on the vehicle and driver that needed to be compensated for as opposed to a track on level ground. Due to this, some drivers were unable to finish even a single set of laps without spinning out during the baseline performance assessment. The secondary effect of the drainage camber was an unevenness reported by all drivers with regards to left- and right-hand turns, with all drivers noting that there was substantial wheel lift occurring with the lighter Epsilon on right-hand turns.

3.6 Track Setup: Double-Inverted Figure Four

The second test setup for the vectored torque system and calibration is the track called the double-inverted figure four (DIFF). A variation on the standard figure four used at UC Irvine for testing acceleration and deceleration of vehicles coming into and out of turns, the DIFF features three left and four right turns of varying radii from 30ft to 10ft in order to fully test the dynamically adjusted torque vectoring system for speed and steering angle adjustment. A picture of the DIFF is shown below in Fig. 10.

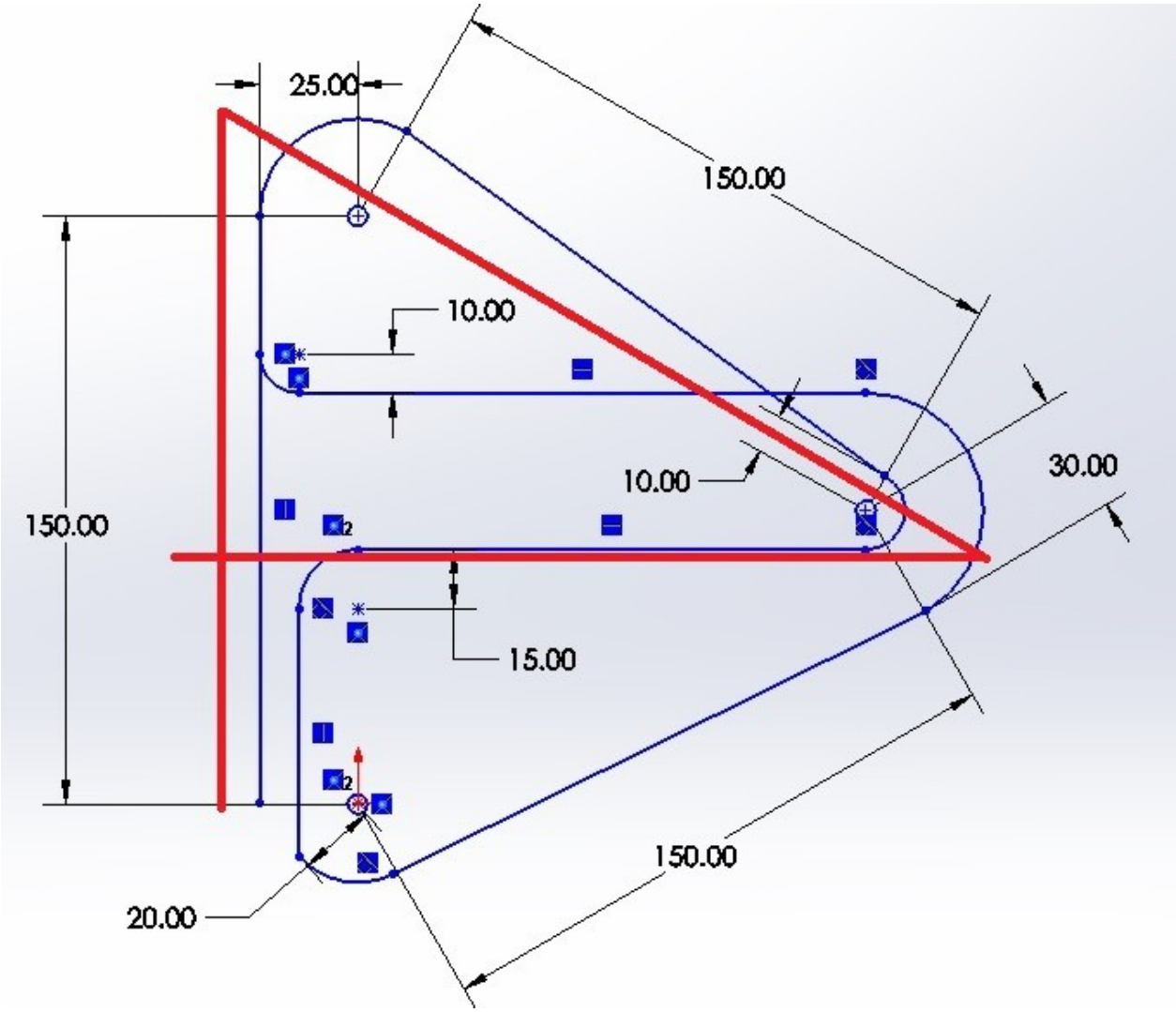

Figure 10: The double-inverted figure four track. Dimensions given in feet.

Highlighted in red in Fig. 10 is the standard figure four track used by the UC Irvine Racecar team for vehicle testing, and includes three straighaways allowing a vehicle to be accelerated into a turn, before coming around a sharp bend around a lamp post. The DIFF, due to the limited space available, superimposes two figure fours on top of each other, with the second figure four being upside-down, hence the name.

The track was designed to test driver and vehicle response to the dynamically adjusting VTS not only as a function of constant turn radius and speed as measured on the skid pad, but also as a function of acceleration and deceleration on corners on a live track. As each turn has a different entrance and exit speed, a longer track will allow for the accumulation of driver history and track history, with the cumulative benefits and errors to the driver visible in the data. Additionally, while the skid pad testing was conducted under "ideal" conditions right at the traction limit - i.e. the driver has had time to adjust the speed carefully and balance it against the vehicle's side-slip over the course of several laps and only has a constant radius turn to worry about - the actual track and the different turn radii on the DIFF will cause drivers to enter turns at non-ideal conditions, such as too high or too low entry speeds which fall off the optimal torque bias curve for speed, turn angle, and applied torque.

The VTS, while tested and calibrated on the skid pad, will have to account for these changed conditions as well, and thus testing a driver under actual track conditions off the ideal curve becomes a necessity to further validate the results and come to a conclusion as to the benefits and drawbacks of the VTS as proposed here. Drivers will dynamically adjust their steering and throttle settings based on the feedback they receive from the car as they make the turns on the track, which adds to the necessary responsiveness of the VTS under actual road conditions.

3.7 Torque Vectoring Phased Testing

Testing was conducted in three phases for each vehicle:

- Phase 1: Baseline testing with a single-throttle assembly. In order to train the drivers and remove hysteresis induced by driver experience, several drivers were trained beforehand on the vehicle in order to familiarize themselves with the way it handles until they could deliver consistent performance on the skid pad runs. This provides a data set to compare the performance changes caused by the torque vectoring system to.
- Phase 2: Static testing with a dual-throttle, set torque bias on the skid pad. By imparting a set bias between the inside and outside wheels for left- and right-hand turns, the optimal setting for best results for time and stability were found and used to calibrate the dynamic setting based on the set radius turn of the skid pad.
- Phase 3: Dynamic testing on the skid pad and double-inverted figure four track in order to assess the viability and effects of the torque vectoring on a series of turns of varying radii and speeds.

Each phase of testing was conducted until the drivers could deliver consistent performance at a given setting. Runs were conducted on the basis of three failure criteria: *irrecoverable failures*, where the driver leaves the course and is unable to recover, *recoverable failures*, where the driver is able to re-establish control and resume the lap, and *recoverable aborts*, where the driver is able to resume, but the run is aborted for safety reasons. While not part of the data set that was used to assess the performance of the vehicle with and without the VTS, these instances were recorded as a metric for the stability improvement or deterioration of the vehicle.

3.8 Data Acquisition

The main data recorded for the experiments was the lap times for both the skid pad and track runs. Skid pad runs were conducted in sets of six, with two recorded but unused laps for warm-up in order to get the driver up to speed, as well as four recorded laps for further data processing. This procedure was put in place due to the need to acquire skid pad data at a fixed vehicle speed, and drivers were unable to reliably reach the set velocity safely without the warm-up laps. Similarly, the lap times for the track were recorded in sets of five laps, with two given as a warm-up and three recorded sets around the 900-ft double inverted figure four track.

Additional data that was recorded was the vehicle's speed, power consumption, total current draw, and instantaneous voltage via the onboard Cycle Analogger datalogging device for power consumption measurement and estimation.

3.9 Summary

Testing was conducted in three phases, with a heavy focus on producing experimental results to test and verify the calculations made in Section 2. Driver training took a significant amount of time initially as procedures were developed. Phase 3 repeated the Phase 2 experiments on the skid pad, attempting to replicate the results as, in theory, on a fixed skid pad at a fixed velocity, the static and dynamic settings are identical. However, it was found that the dynamic VTS was beneficial to the drivers adjusting when faced with uneven road surfaces or temporary loss of traction.

Due to the nature of the experiment, the raw data recorded is only one part of the total information gathered. Anecdotal notes and feedback from drivers with regards to individual laps were also recorded and taken into account and considered.

4. Torque Vectoring Experiments

4.1 Introduction

Phase 2 and 3 experiments are based solely on the quantification of the effects of the vectored torque system on the vehicle's performance on the skid pad and track. as such, offset values were calculated as follows in Table 4 for the Phase 2 testing, and implemented in order to bracket and determine the optimal setting. It was also investigated whether this optimized setting corresponded in any way to the unloading on the inside tyre calculated in Eqn. 3 and as such, whether this was an accurate way of estimating the preliminary setting for a vehicle's torque vectoring based solely on the chassis properties. The offset resistance noted in Table 4 is the equivalent of the R_1 offset resistance in Fig. 4-B, which, together with the steering input comprises the adjusted parallel input to the throttle T1-B and T2-B, respectively.

Table 4: Torque vectoring settings.

% Torque Bias	Offset Resistance (kΩ)	Notes
0	0	
10	0.53	
25	1.43	
40	2.5	
50	3.33	
55	3.79	Predicted optimal for Epsilon
66	5	Predicted optimal for Gamma
75	6	
86	7.5	
100	10	Baseline (solid axle)

For the purposes of this thesis, the percentage of torque bias given is the amount of torque on the inside wheel with respect to the torque on the outside wheel, that is, 100% torque bias would mean that the inside wheel has the same amount of torque applied to it as the outside, while 10% would mean that the inside has 1/10 of the outside torque.

4.2 Theoretical Torque Differential

The possible torque vectoring settings for Phase 2 and 3 were calculated as a linear function of the throttle resistance and torque bias setting according to Eqn. 4 from Fig. 4:

$$P_{inside} = P_{outside} \cdot R_{equiv} \cdot [(1/R_{throttle}) + (1/R_{TV})]^{-1} \quad (4)$$

The inside wheel power is thus calculated as per the circuit setup as a function of parallel resistances, allowing for an asymptotic response as the torque bias approaches 0%, shown below in Figs. 11 and 12.

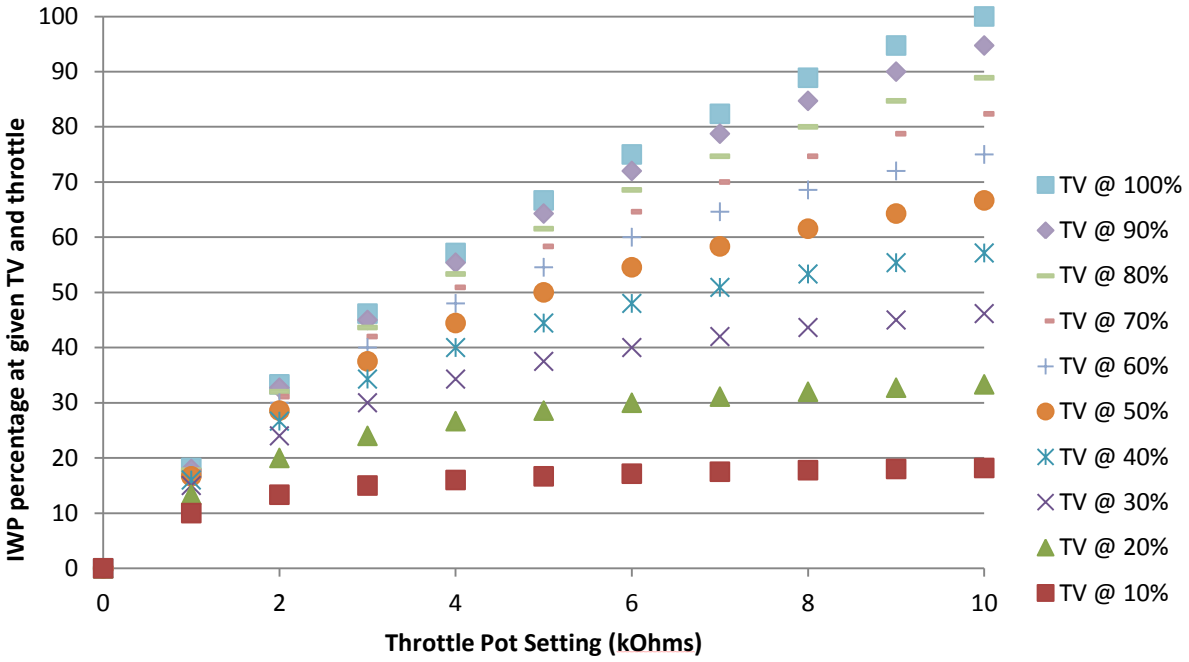

Figure 11: Static torque vectoring setting as a function of throttle.

The amount of potential reduction of the inner wheel torque is clear; however, it should be noted that the torque bias setting does not actually fully correspond to the applied throttle. The response is set such that at half-throttle, the response matches the set torque reduction, while at higher speeds, the torque reduction is more limited in order to allow for a more responsive throttle. On the static skid-pad, at a single given turn radius and - ideally - a single speed, this

will allow for testing and quantitative comparison of the performance of a torque-biased motor setting with regards to a solid-axle equivalent drive.

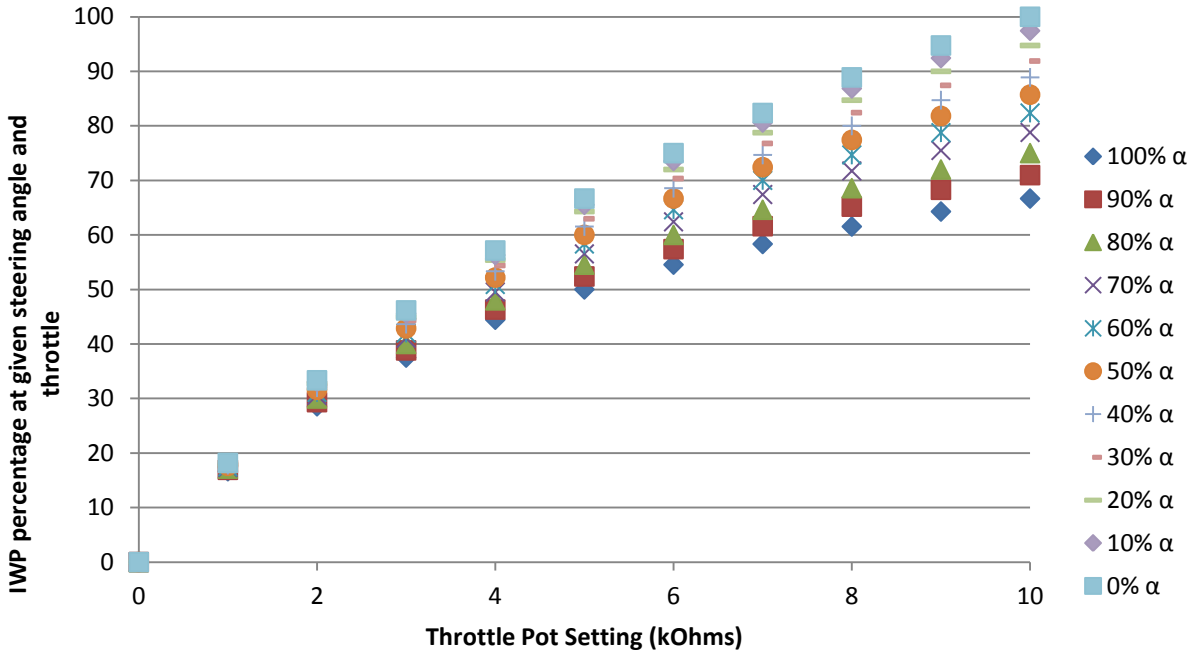

Figure 12: Dynamic throttle differential for various steering angles.

Figure 12 is the result of the same calculation for a given number of steering angles after calibrating the given steering linkage travel to the 10-cm potentiometer. Once the steering input is mapped into what for Fig. 11 was R_{TV}, the inside wheel torque output can be plotted as a function of both R_{TV} and $R_{throttle}$. The result is that due to the dependency on both the throttle and steering inputs, the system allows for full throttle displacement at zero steering angle and will match the throttle signal closely at low speeds. As such, the throttle response is designed in a manner that for high-speed, but shallow (low α) turns, the torque reduction on the inside wheel is mitigated, while for high-speed, but narrow (high α) turns, the response can be set to a designed reduction based on the skid pad data.

The result of the dynamic circuit setup is a system that can accept an input offset value and thus determine an output range of torque bias values for a given system based on the current steering angle and throttle position, allowing for dynamic, real-time adjustment beyond a simple static bias system based on steering angle only.

4.3 Data Reduction: Skid Pad

Date reduction of the skid pad and track results were performed by graphing the resulting lap times per driver, turn direction, and torque vectoring setting, and comparing them to each other as well as the baseline over the course of the day. Fig. 13 shows the baseline runs for the skid pad that were recorded during driver training, as the drivers acclimatized themselves to the vehicles in order to produce consistent lap times.

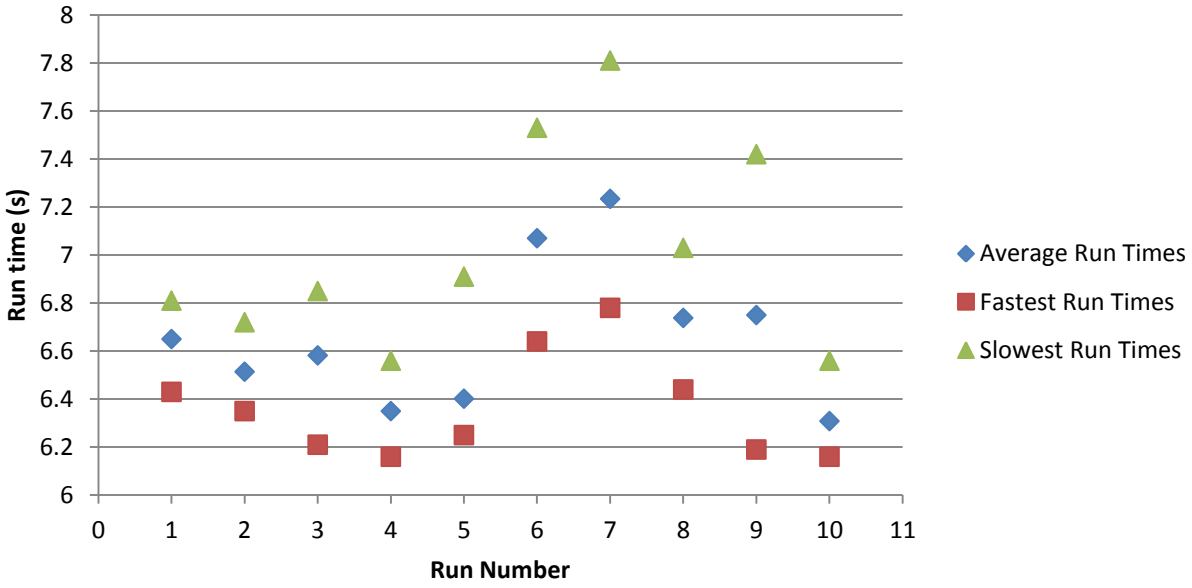

Figure 13: Driver training skid pad runtime overview. Driver: Jay. Car: Gamma.

Skid pad times were plotted along with their averages, fastest, and slowest times, and outliers were filtered out as per the experimental notes due to drivers losing control momentarily and leaving the skid pad during a single lap (as per the recoverable failure state), but recovering

enough to finish the set. Fig. 13 shows that as time goes on, the driver performance changes as the individual driver familiarizes himself with the upper limit of the car. In this case, the driver started out quickly and attempted to go faster, resulting in more oversteer and loss of control before eventually reaching a plateau, at which point consistent data sets could be recorded for further processing.

Fig. 14 shows a comparison of the driver times with torque vectoring settings against the baseline for Gamma for one of the drivers, along with the calculated error bars.

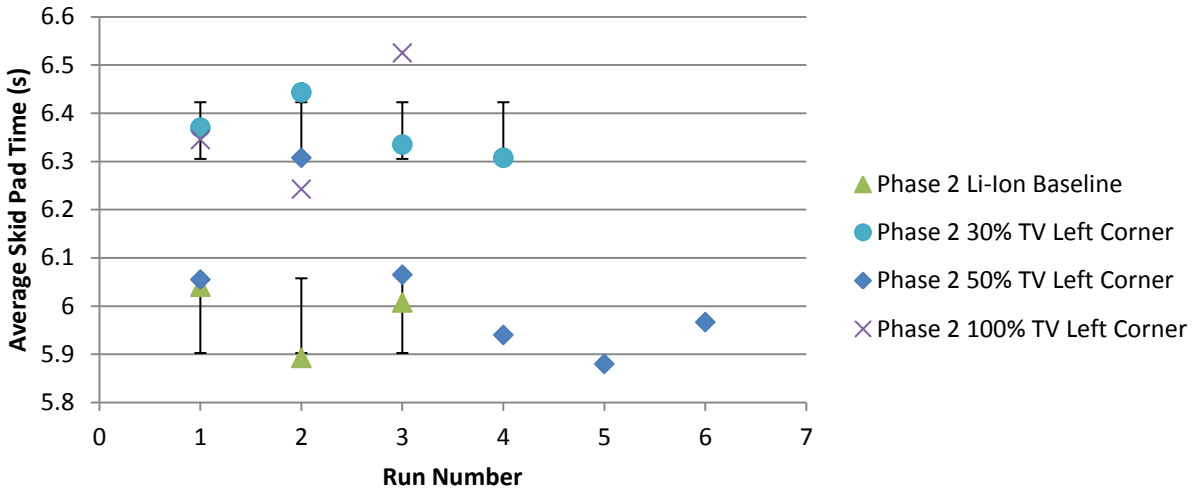

Figure 14: Torque vectoring skid pad times. Driver: Jay. Car: Gamma.

4.4 Summary

Data reduction for the raw lap times was conducted by filtering out the outliers as per the experimental notes based on recoverable failures, as the driver had left the track, but was able to recover. Average and detailed histograms were generated in for all torque bias settings in order to assess the performance of a driver for a given setting over time with the standard error calculated for each set of laps.

5. Static and Dynamic Torque Vectoring Results

5.1 Introduction

Based on Eqn. 3, the calculated expected optimal torque percentage on the inside wheel for Gamma and Epsilon on the skid pad were computed as 66% for Gamma and 55% for Epsilon, respectively. Using the calculations for the throttle and offset potentiometers (Figs. 11 and 12), the correct setting could be found and tested for both performance and stability. The experimental results were then used to verify the calculation. It was found that for Gamma, the effect of mitigating oversteer was more pronounced than any improvement over the baseline lap times, while for Epsilon the improvement in lap times was much more evident.

5.2 Overview of Results

The results suggest that the torque vectoring does have a significant effect on the vehicle's driving characteristics; in the extreme case of Gamma, the car could be tuned from heavy oversteer to neutral, and showed a significant improvement when the VTS was active in a neutral setting. Epsilon showed a smaller but more consistent margin of improvement, likely due to the better chassis characteristics with regards to turning. The torque vectoring in some cases matched or exceeded the baseline capabilities of the test vehicle despite the fact that it effectively diminishes the total power available, but at a significant improvement in stability and controllability as displayed in Table 5.

Table 5: Gamma controllability results.

	Number of Runs	Irrecoverable Failures	Percentage
Baseline (100%)	80	27	34%
Phase 2 0%	24	14	58%
Phase 2 50%	24	6	25%
Phase 2 70%	46	0	0%

As Table 5 illustrates, Gamma, due to its mass, is relatively stable even in its oversteer. However, as the torque bias is set to 0%, which is no power on the inside wheel, causing the inside to drag along, the vehicle suddenly becomes unstable, causing a large number of spin-outs. The trend follows with increasing torque vectoring setting that as the bias causes the vehicle to oversteer less, it settles and becomes more stable. At the baseline, however, the vehicle again exhibited heavy oversteer due to the inside wheel torque exceeding the traction limit and inducing wheel slip.

It was also found that due to the net loss in power of as much as 50% of the total applied engine power (at 0% torque bias) to, on average 25% power loss (at 50% torque bias), the torque vectored vehicles rarely exceeded the baseline times. However, as vehicle stability improves with the torque bias setting, skid pad times began matching the baseline results.

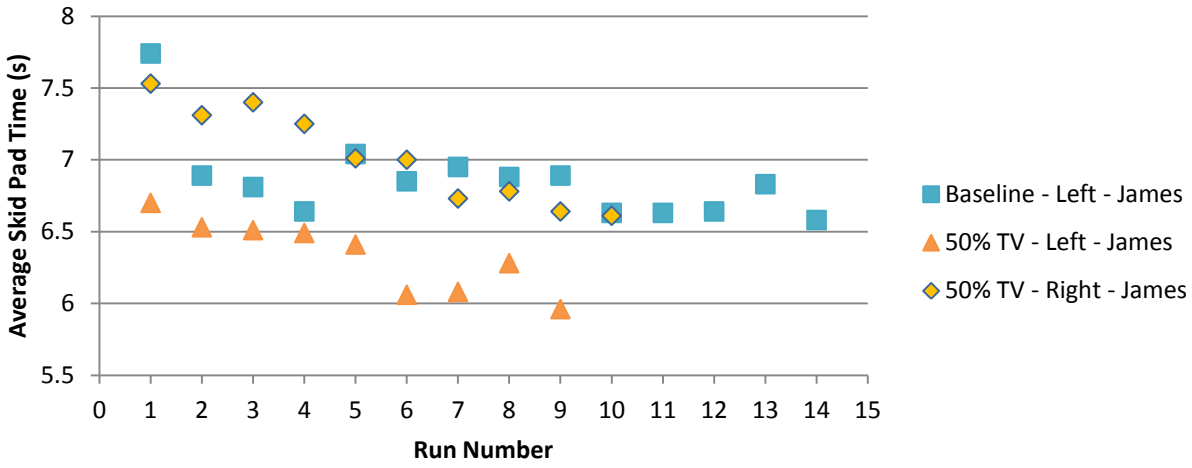

Figure 15: Skid pad results for the most inexperienced driver. Driver: James. Car: Epsilon.

Epsilon, overall, yielded very little results in terms of stability improvement, as most drivers were fully able to keep control of the car without completely spinning out, except for the most inexperienced of the group, who was able to retain full control with the torque vectoring system turned on during right-hand turns, but had been unable to complete a single lap without

spinning out before, as shown in Fig. 15. One of the reasons for this differential was noted by all drivers as the uneven surface of the skid pad, which posed more problems turning right, due to the drainage camber causing wheel-lift, than when turning left.

5.3 Baseline Skidpad Results

The baseline for both cars were taken using four different drivers; one for Gamma and three for Epsilon. The overall results are shown in Figs. 16 and 17 for the left- and right-hand turns, respectively, for all drivers.

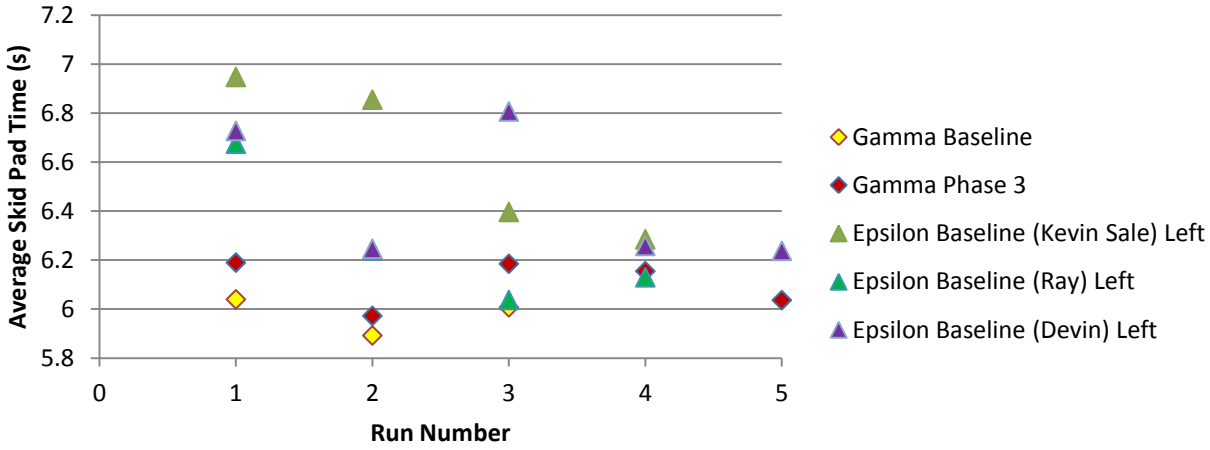

Figure 16: Left-hand turn average skid pad baseline times.

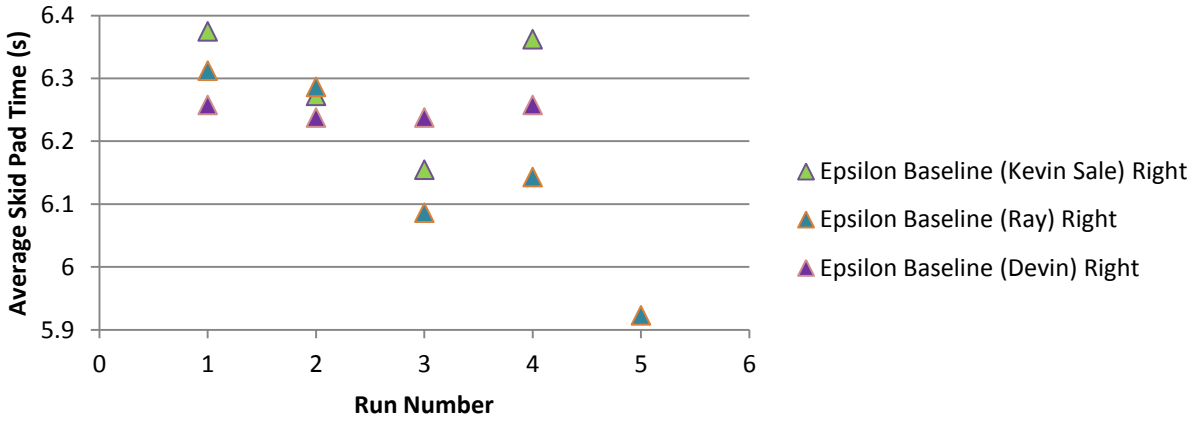

Figure 17: Right-hand turn average skid pad baseline times (Epsilon).

Fig. 18 shows a left versus right comparison of the skid pad times for Epsilon for one of the drivers. Due to the uneven nature of the skid pad, most drivers found it easier to turn left rather than right, however, the right-turn skid pad times indicate that, while drivers were overall more comfortable turning left, skid pad times were on par with each other.

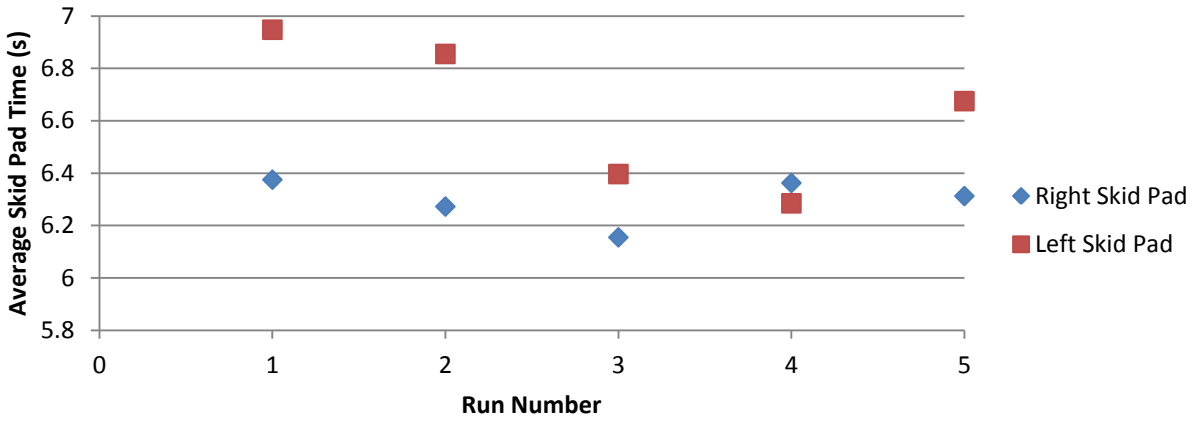

Figure 18: Left vs. right skid pad times. Driver: Kevin Sale. Car: Epsilon.

Despite their very different driving characteristics and chassis specifications, both vehicles, on average, perform similarly on the skid pad and in the long term, driver training managed to cancel out the left-to-right bias when turning the vehicle.

5.4 Static Torque Vectoring Results

Once the baseline testing was completed and the drivers had sufficiently familiarized themselves with the vehicle, static testing was commenced. Unfortunately, due to circumstances causing Gamma to be dismantled before testing could be completed, data was only acquired for this test vehicle on left-hand turns. Fig. 19 shows the Phase 2 static torque bias test results for Gamma for the main driver.

The zero setting, that is, the equivalent to an open differential, yielded the worst and most unreliable results, as corroborated by the drivers' feedback. The 50% setting yielded the best

performance, matching up close to the baseline performance of the vehicle; however, the 70% setting resulted in the highest stability for the vehicle. As such, a medium between the two was chosen for proceeding into Phase 3, at the calculated theoretical optimal for the car at 65%.

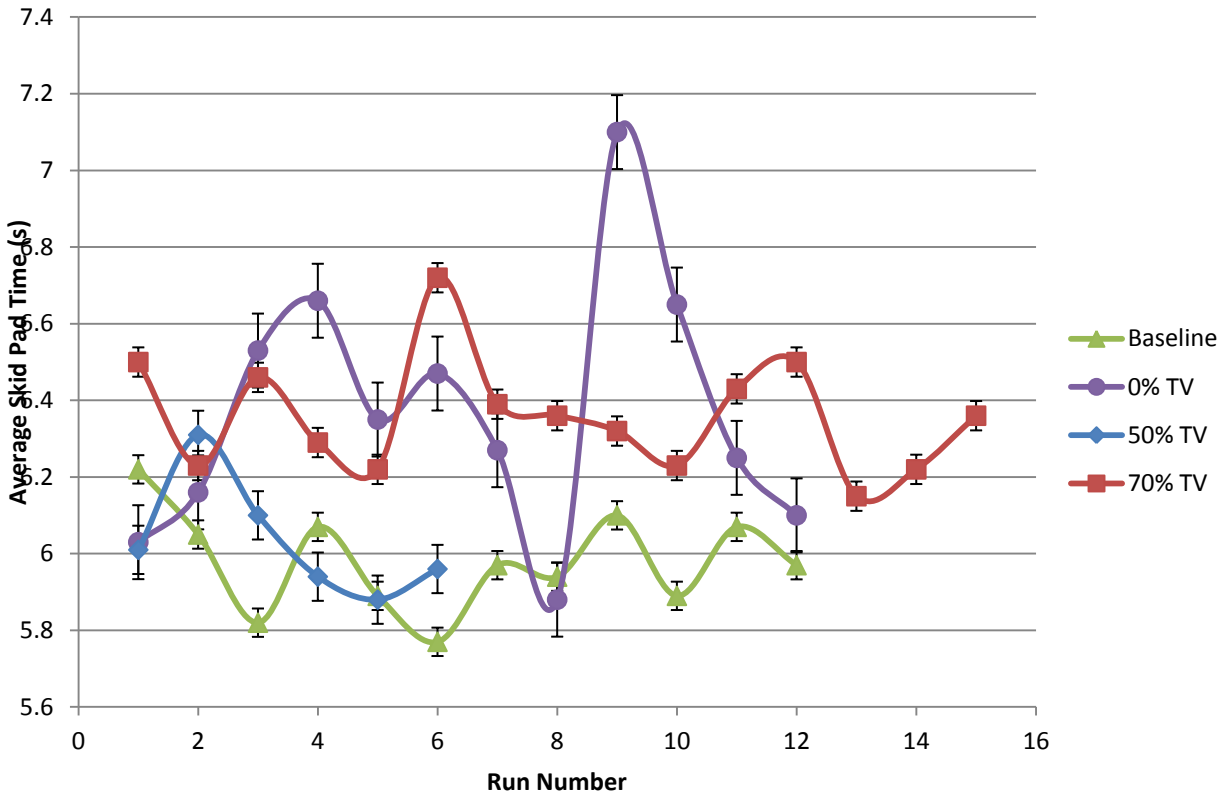

Figure 19: Skid pad results at various torque bias settings. Driver: Jay. Car: Gamma.

Figs. 20 and 21 show two drivers' results for Epsilon, allowing for comparison of the baseline to static setting performance. Fig. 20, in particular, is an excerpt from one driver's data sample for left-hand turns and displays the difference between the vehicle's performance with the VTS on and off, with the system set at the estimated optimal for Epsilon, at 55%. There is an average of 0.2725s improvement across all skid pad runs with the torque vectoring system active, which is well outside of the standard error for the sample taken.

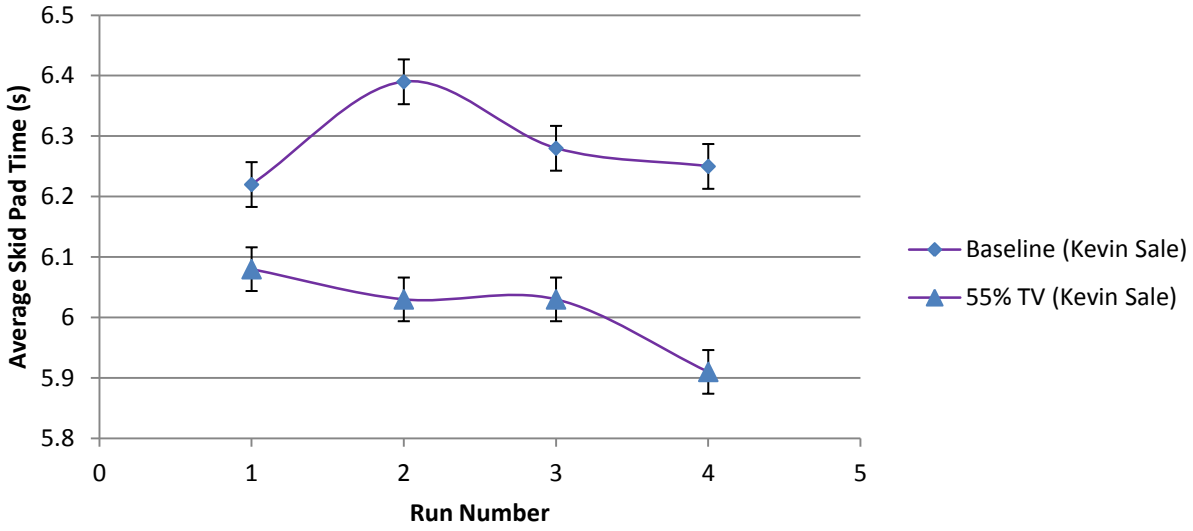

Figure 20: Baseline vs. theoretical optimal left-turn skid pad result over two sets. Driver: Kevin Sale. Car: Epsilon.

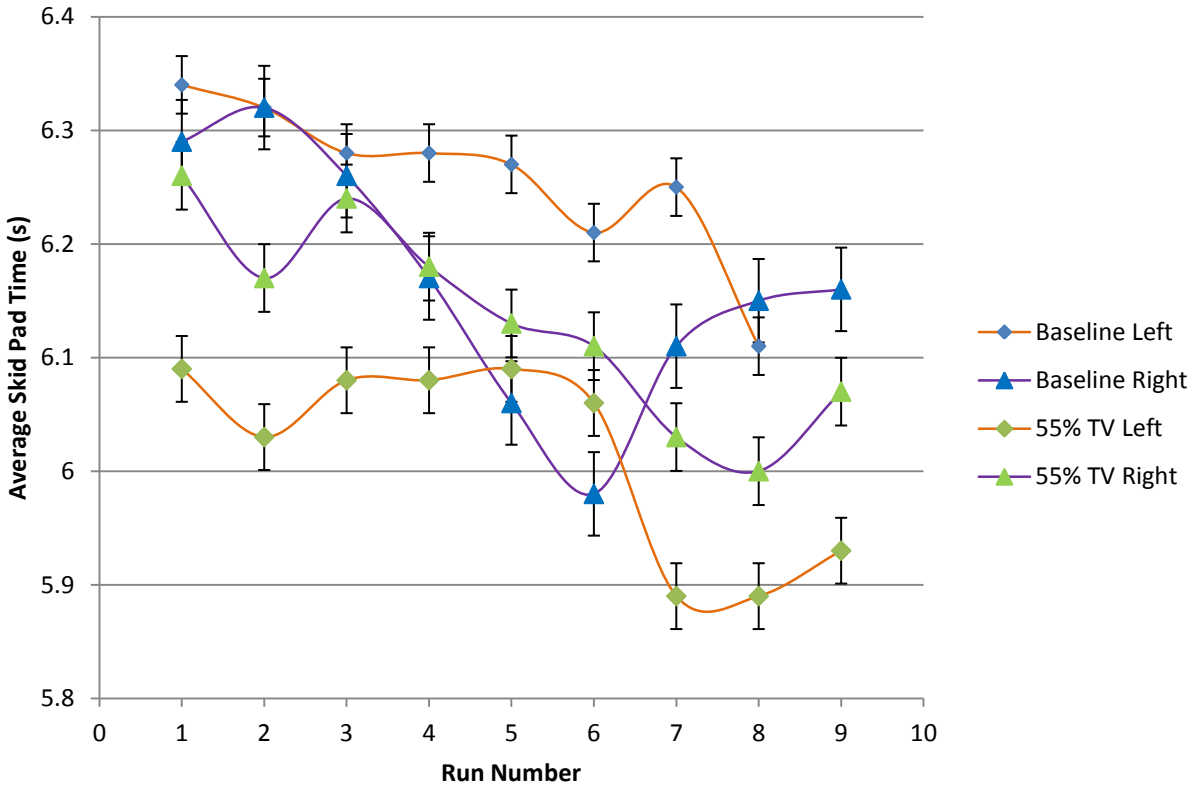

Figure 21: Baseline vs. theoretical optimal skid pad results. Driver: Ray Molina. Car: Epsilon.

As Fig. 21 shows, the skid pad times with the VTS for left-hand turns are consistently faster than the baseline measurements, while right-hand turns, with two exceptions, follow the same trend. It was shown that it is possible to attain equal lap times with the solid-axle setup, that is, without the torque vectoring system. However, according to driver feedback, it was more difficult to control the car and adjust for sideslip at such speeds, indicating that the vehicle is reaching its traction limit. The results of Fig. 20 and 21 came from a blind test, with the drivers unaware if the VTS was turned on or off. Feedback from drivers after each set indicated that they noticed a difference in the handling of the vehicle, however.

A more detailed study of the torque vectoring effects is shown in Fig. 22-25, broken up by driver and turn direction, with data points shown at major torque vectoring settings of 10% (corresponding to high oversteer on Epsilon), 50% (neutral, neither understeering nor oversteering tendencies), and 75% (moderate understeer), as well as the baseline, which the drivers regarded as highly understeering.

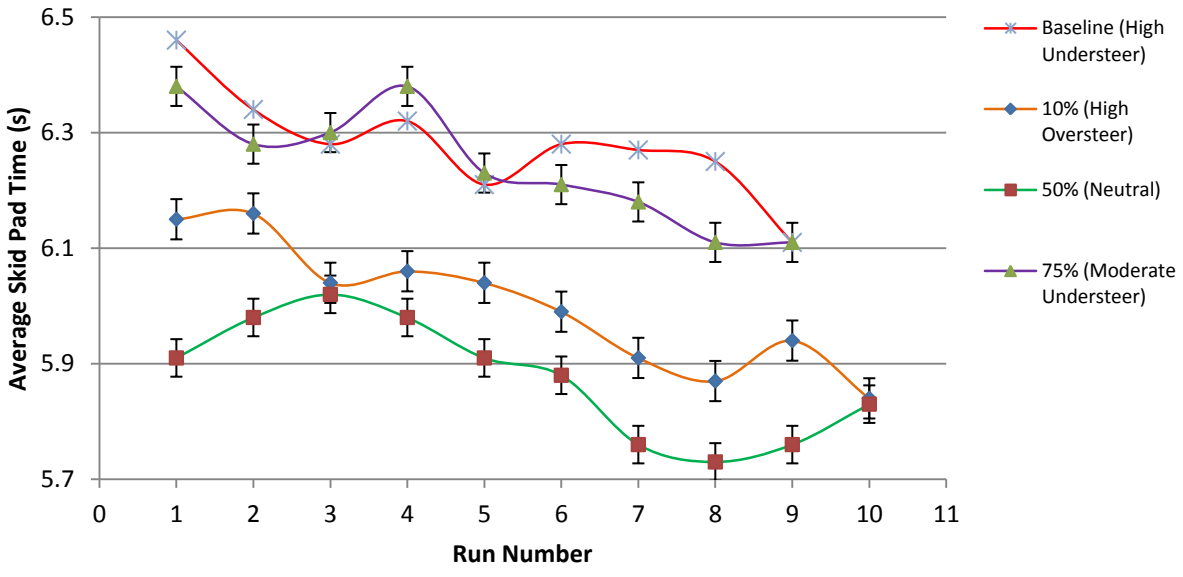

Figure 22: Skid pad times by driver and direction, left turn results. Driver: Ray Molina. Car: Epsilon.

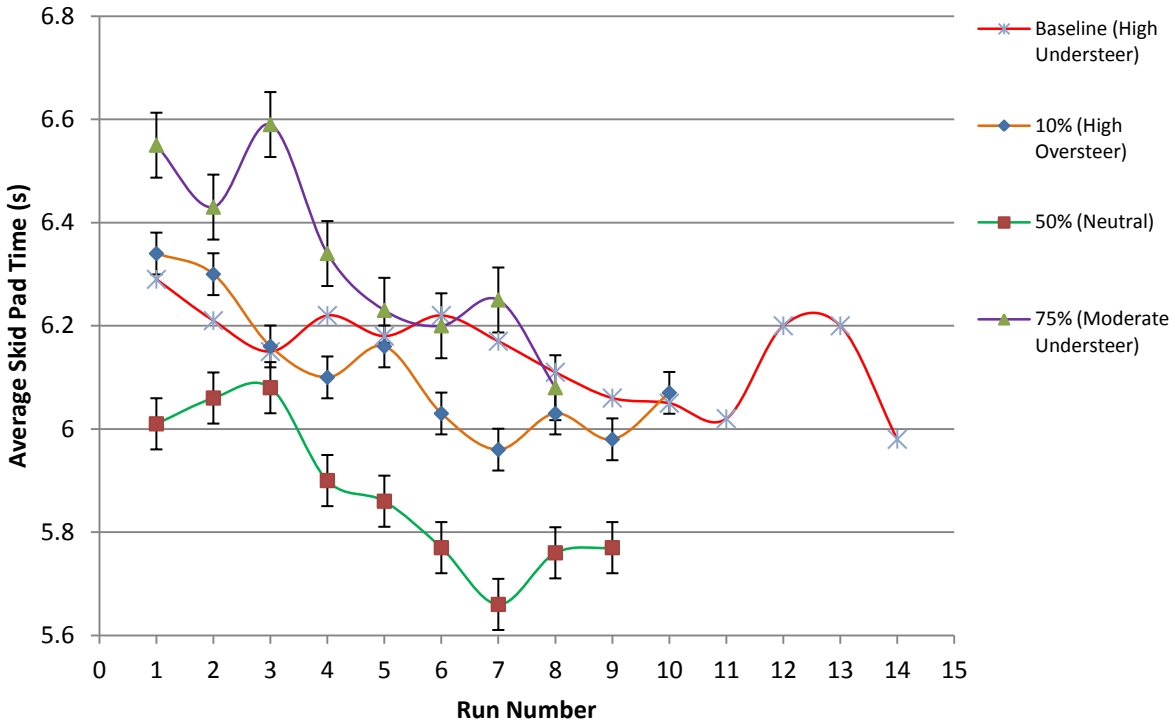

Figure 23: Skid pad times by driver and direction, right turn results. Driver: Ray Molina. Car: Epsilon.

Figs. 22 and 23 illustrate that for left-hand turns, the baseline and 75% setting were nearly identical in terms of skid pad performance. However, both the neutral and oversteer settings (50% and 10%) yielded better results than the baseline, with the neutral setting performing slightly better. The skid pad times for right-hand turns show more variation due to the surface conditions. Still, the understeer settings yield similar results, with the high oversteer setting only seeing a slight improvement of an average of 1/20 of a second.

It is for right-hand turns, however, that the neutral 50% setting yields the best results as, according to driver feedback, controllability of the vehicle was improved over the sections where wheel lift occurred.

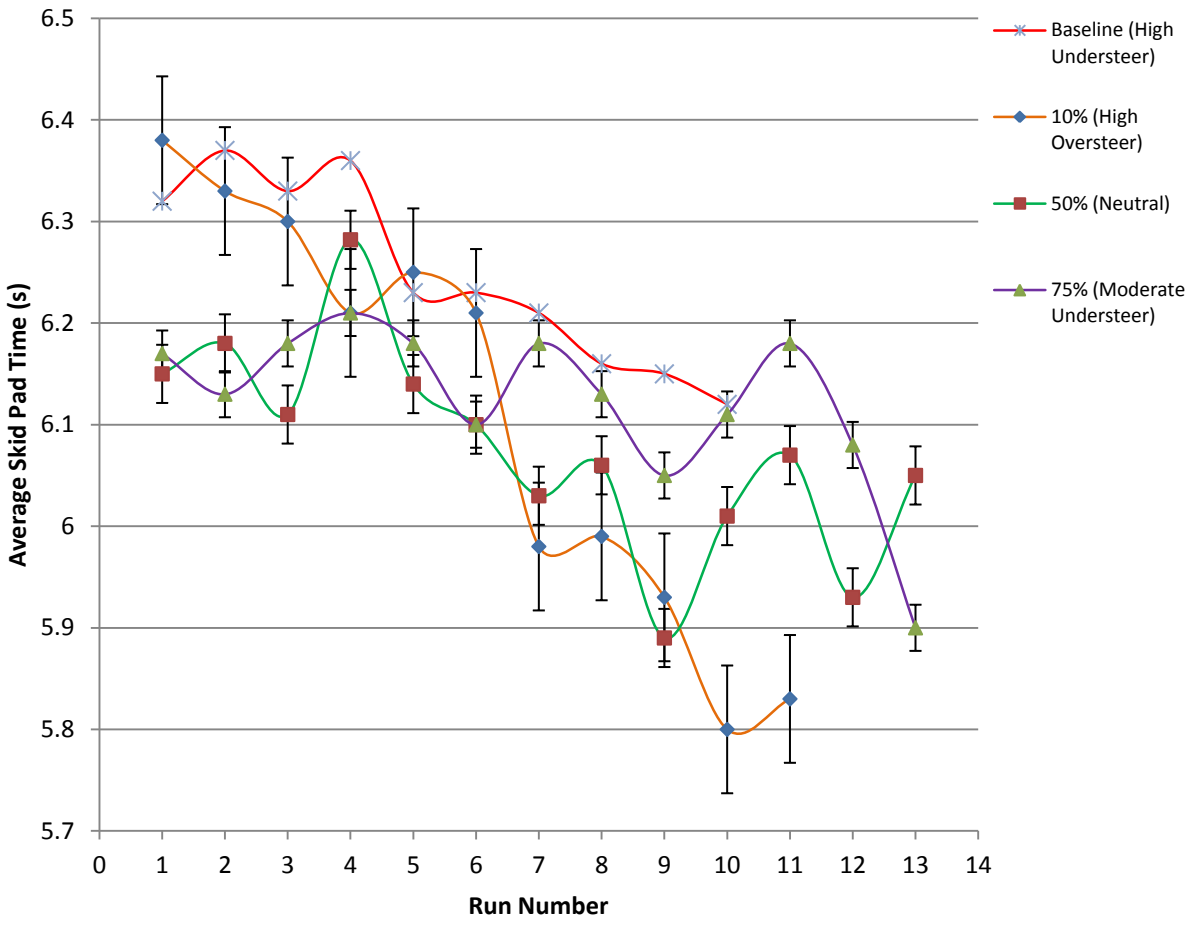

Figure 24: Skid pad times by driver and direction, left turn results. Driver: Devin Staal. Car: Epsilon.

Fig. 24 shows the same left-hand turn graph for a different driver at the same four torque vectoring settings. While the best results were achieved with a highly oversteering setting at 10%, the second driver's results are less clear than the first. The torque vectoring results, however, for the neutral setting are consistently better than the baseline, though sometimes overlapping within the error band.

Fig. 25 shows the same results for the right-hand turn for the second driver, which yielded a much clearer segregation of torque vectored and non-torque vectored performance. The

baseline suffered from severe wheel lift and control issues, as indicated by the driver's feedback and reflected in the skid pad times. However, it should be noted that for the more unstable right-hand turn, any measure of torque bias aided in the stability of the vehicle, though as with the left-hand turns, for this particular driver the optimal setting could not be found due to the close proximity of the measured performance.

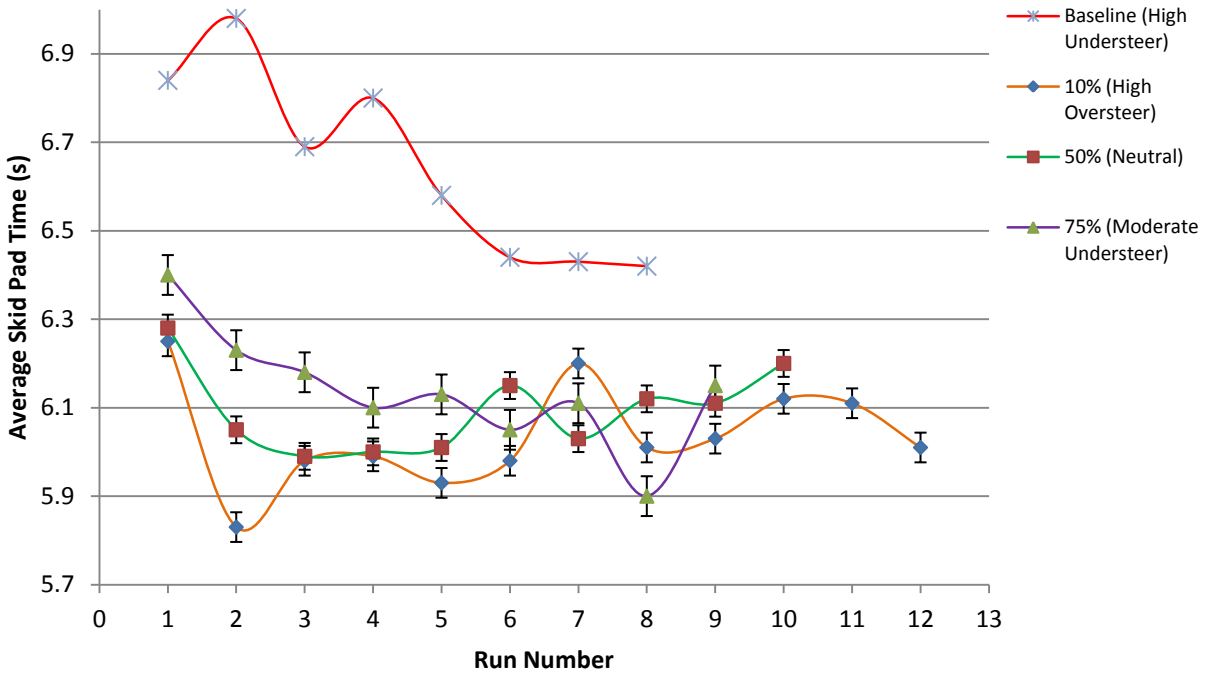

Figure 25: Skid pad times by driver and direction, right turn results. Driver: Devin Staal. Car: Epsilon.

Figs. 26 and 27 offers a more detailed look at the left and right variations on Epsilon for both drivers using the baseline and the neutral setting. The first driver, whose data is shown in Fig. 26, is an experienced driver, while the driver of Fig. 27 is a novice driver. Both noted an increase in controllability with the torque bias active over the baseline, and indicated that the vehicle, especially during the warm-up laps, suffered from heavy understeer and later wheel lift during right-hand turns.

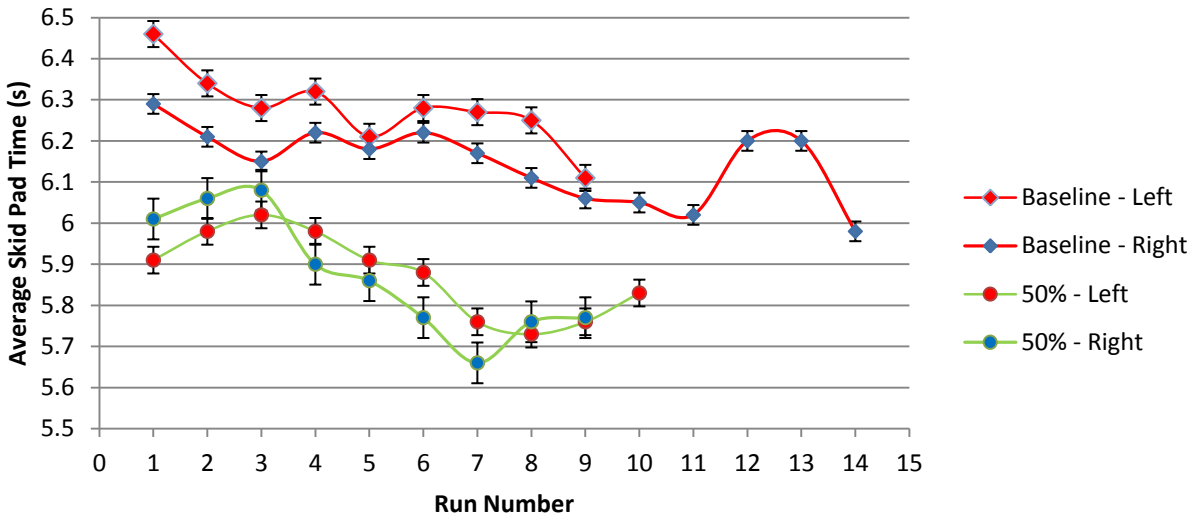

Figure 26: Left-to-right skid pad comparison. Driver: Ray Molina. Car: Epsilon.

In the case of Fig. 26, the times for this driver between the left and right skid pad times are comparable and within the standard error of each other for both the baseline and the neutral torque vectoring setting. In both cases, there is a significant and consistent improvement in the vehicle's skid pad performance with the torque bias active. Fig. 27 shows the same comparison for the second driver:

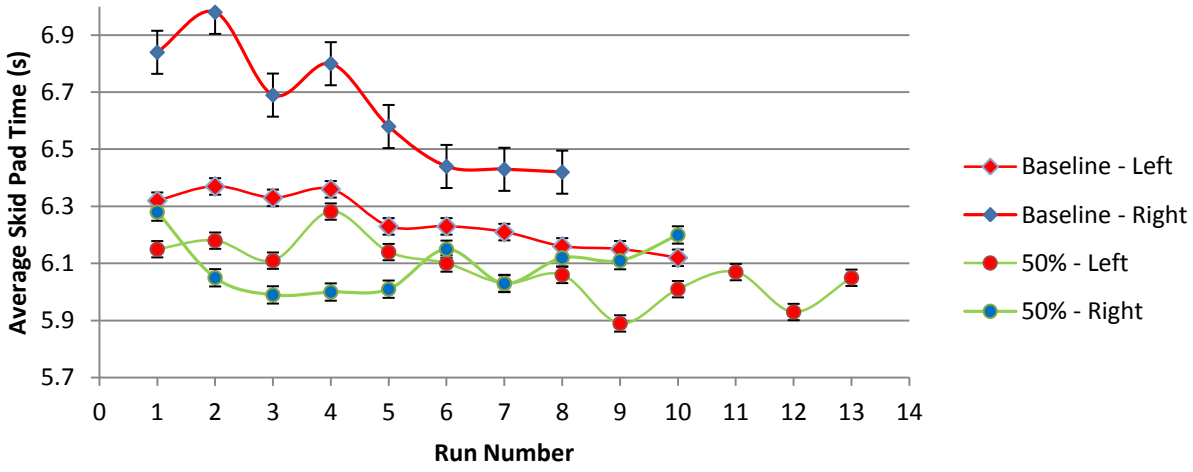

Figure 27: Left-to-right skid pad comparison. Driver: Devin Staal. Car: Epsilon.

In the case of the second driver, there is a significant difference between the left and right skid pad times for the baseline measurements, as the right-hand turn baseline measurements are up to one-half second apart. However, with the torque bias active, the measured skid pad times for right-hand turns approach the 6.0 second margin, while the left-hand turns yield a slight improvement just outside of the error band. In both cases for left- and right-hand turns, the skid pad times with the torque bias active are consistently below the baseline time, though by not as large a margin as for the first driver in Fig. 26.

Fig. 28 below is a graph of a third driver, the most inexperienced of all of the test drivers that volunteered. There is no baseline measurement for right-hand turns, as this driver in nine attempts was unable to complete a single baseline set due to repeated loss of control. A second attempt at taking baseline measurements, after he had successfully completed skid pad runs for left-hand turns as well as with the torque bias system active ended in the same manner.

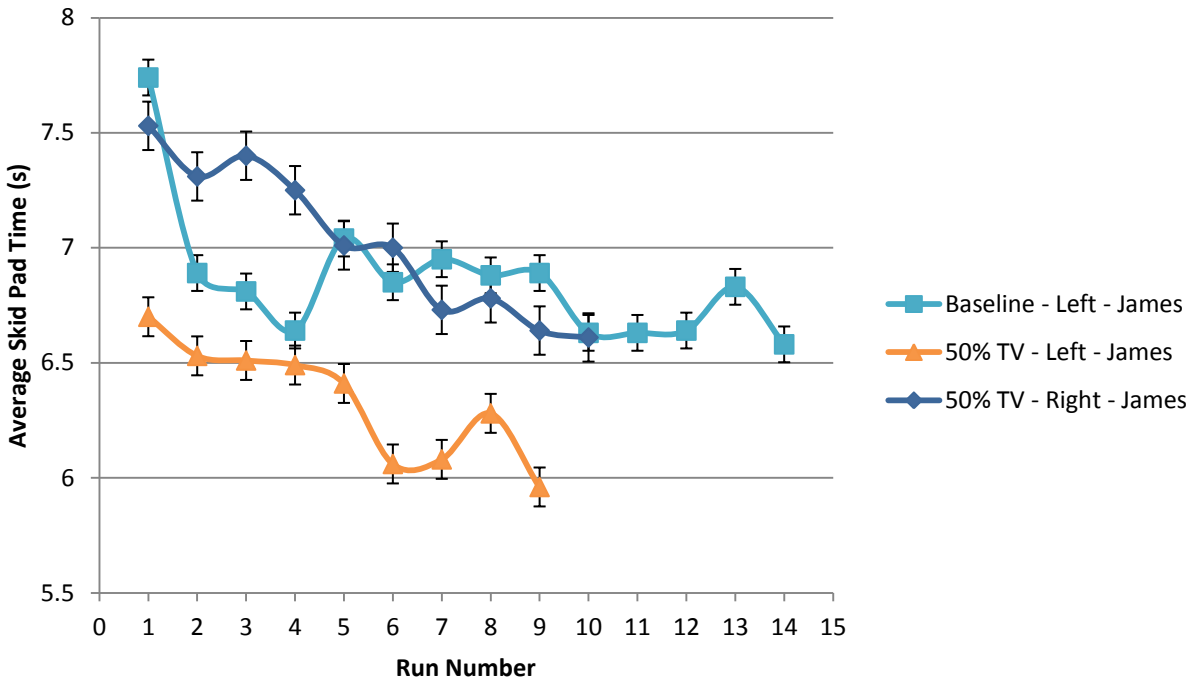

Figure 28: Skid pad results for left- and right-hand turns. Driver: James. Car: Epsilon.

While the torque bias system cannot be assessed with respect to performance improvements for right-hand turns, as there was no baseline that could be measured, the driver noted that vehicle stability was much improved to the point that he was capable of finishing a set of laps whereas without he had been unable to complete them without losing control of the vehicle and leaving the track. With the torque bias active, the right-turn lap times equaled the left-turn baseline, while the left-turn lap times improved significantly, a trend shown by the other novice driver in Fig. 27.

Unlike Gamma, where the stability of the vehicle could be assessed by the number of occurring failures by drivers leaving the track or needing to abort the run, Epsilon had only one driver for whom this was an issue - the novice driver whose data is shown in Fig. 28. As no other driver incurred an irrecoverable failure state, the same measure for Gamma that was used based on Table 5 could not be used. In Gamma's case, while a 50% setting yielded the best lap times while a 70% setting resulted in the fewest triggered failure states, and as such, a medium was chosen to proceed to Phase 3 with. In the case of Gamma, a 65% nominal torque bias was chosen for the skid pad turn angle, as it fell within the control-to-speed margin afforded by the data.

The same analysis is not possible for Epsilon as shown in Table 6, however, as except for one driver, none of the others incurred any irrecoverable failures. Therefore, a further experimental approach was taken in order to determine the accuracy of the calculated optimal setting of 55% and the change in performance between the calculated 55% and the measured 50%.

Table 6: Epsilon stability results.

	Number of Runs	**Irrecoverable Failure States**	**Percentage**
Baseline (100%)	70	9	13%
Phase 2 10%	20	0	0%
Phase 2 50%	20	0	0%
Phase 2 75%	20	0	0%

Figs. 29 and 30 display the results from a fourth driver, and investigate the results of fine-tuning the VTS setting. While 50% is considered neutral for the vehicle, preliminary calculations using Eqn. 3 showed that the optimal theoretical load transfer and thus torque reduction on the inside tyre would be 55%.

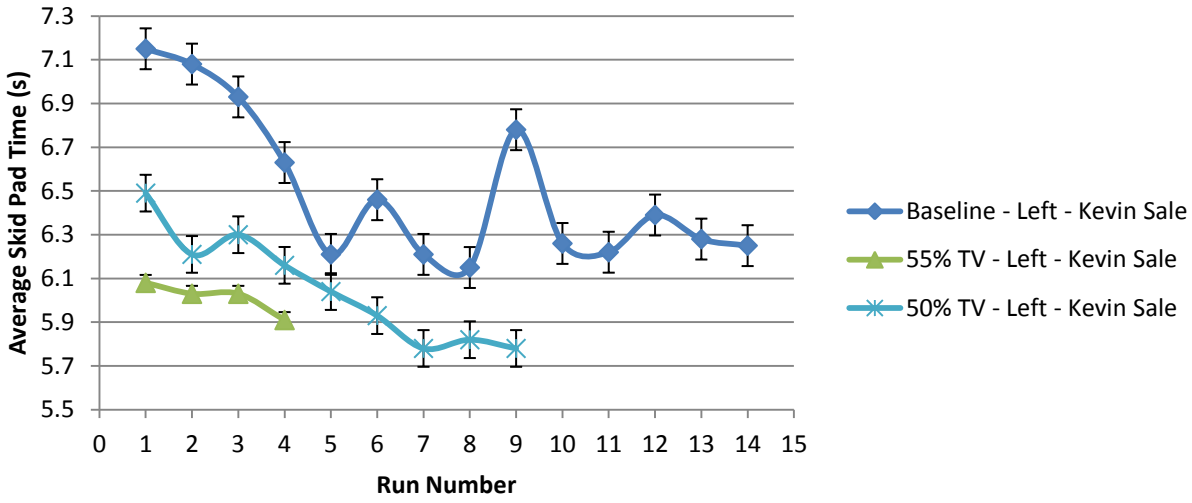

Figure 29: Left-turn skid pad results. Driver: Kevin Sale. Car: Epsilon.

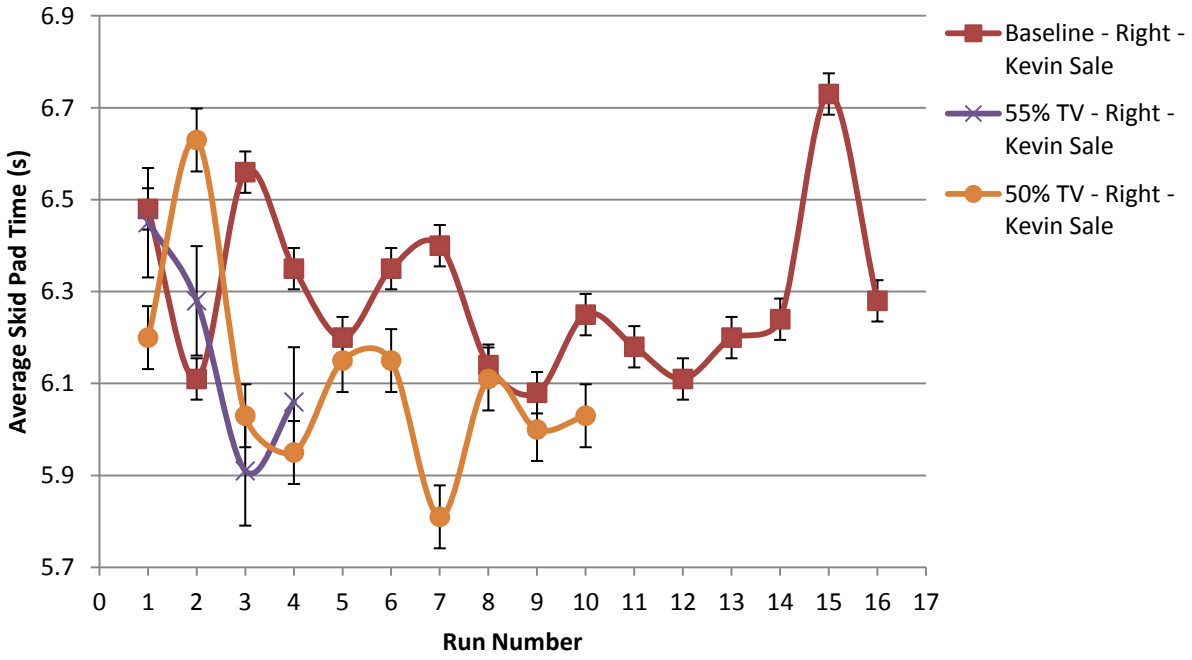

Figure 30: Right-turn skid pad results. Driver: Kevin Sale. Car: Epsilon.

As Fig. 29 shows, both the 50% and 55% torque bias setting consistently result in a faster skid pad time, as well as mitigating control issues. The 55% setting on average results in even better performance. Fig. 30 displays the same data for right-hand turns.

Unlike the left-turn results, right-hand turns yield much less reliable and more erratic data due to the uneven surface of the track. However, it should be noted that despite the fact that on Gamma, the VTS caused a net power drop, this has not has as visible of an effect on Epsilon, where even with a significant drop in net power (up to 25% of the total applied power and torque, due to the 50% drop of inside torque), the skid pad times have been equal or better than the baseline times on Epsilon, barring control issues that were noted by the drivers.

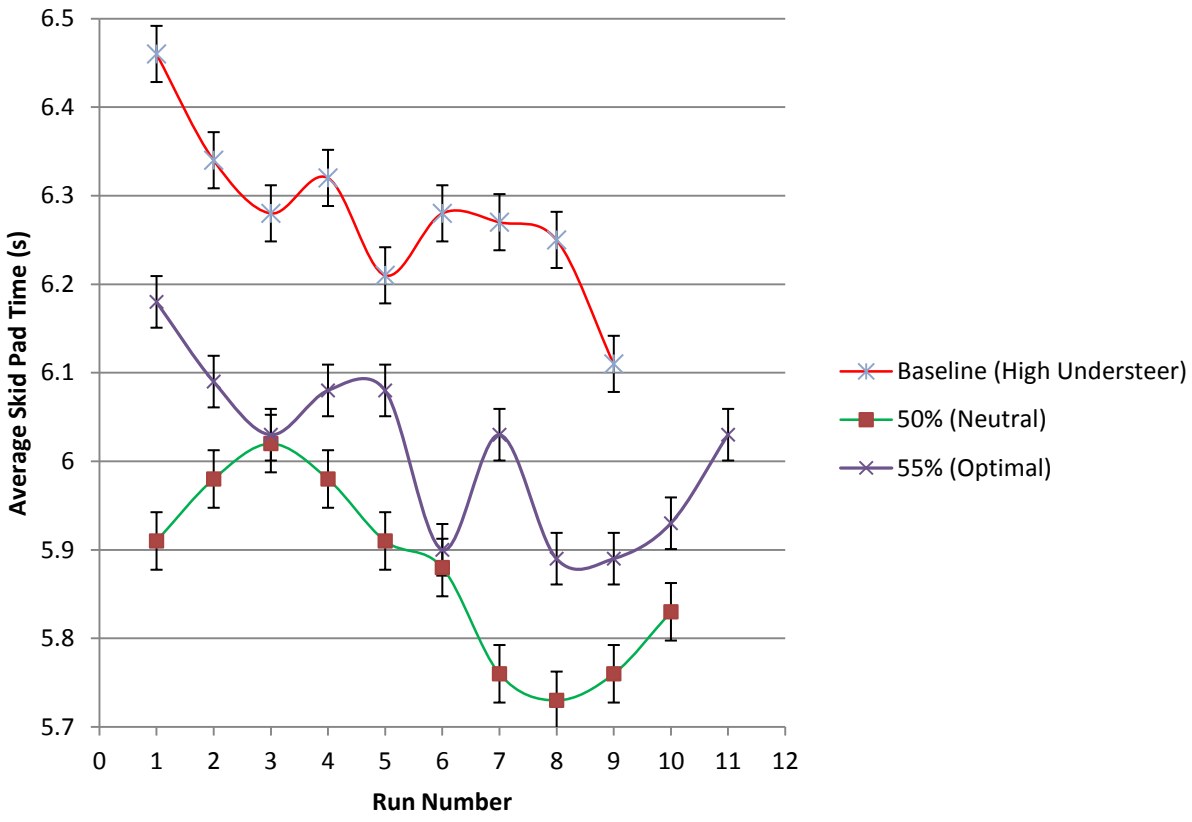

Figure 31: Left-turn torque vectoring fine tuning. Driver: Ray Molina. Car: Epsilon.

Figs. 31 and 32 show the same results for the primary driver of Epsilon, and compare the improvement of the 50% to the 55% setting. In the case of this driver, the 50% setting was more effective for both turn directions, though it still yielded a performance increase over the baseline.

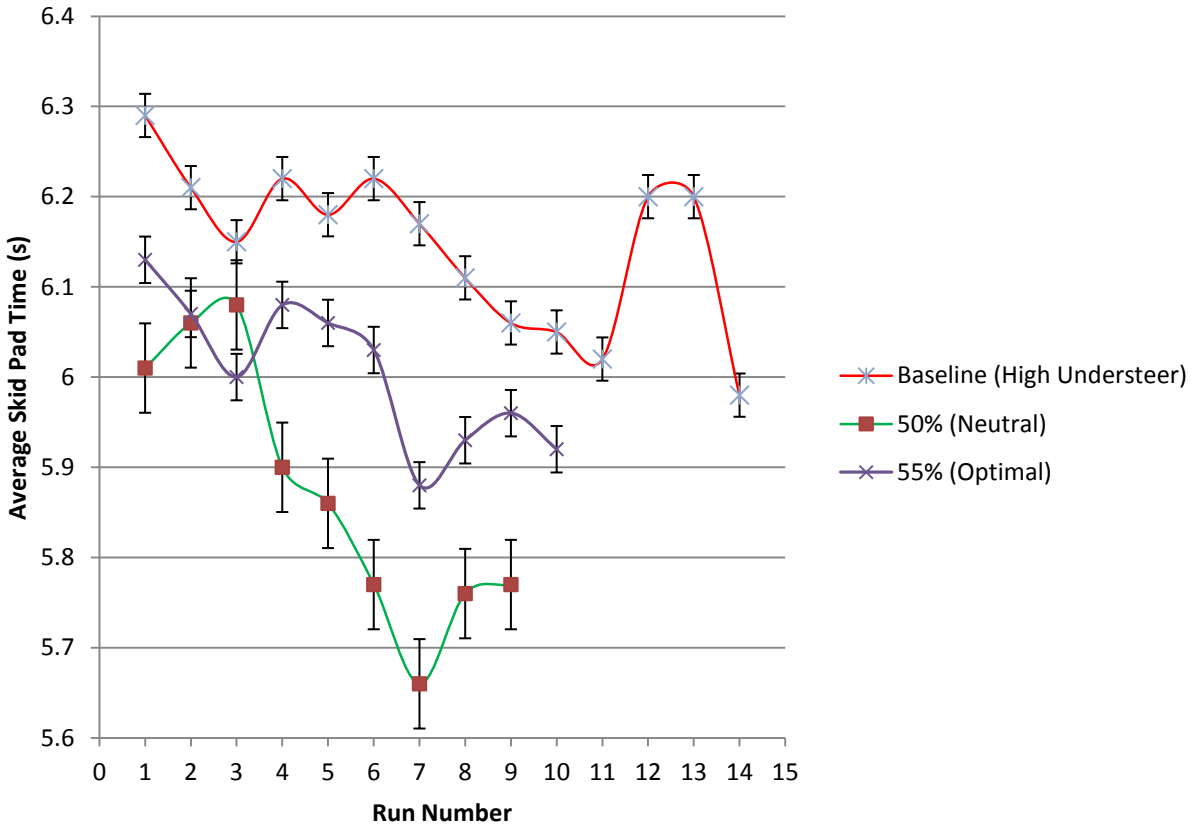

Figure 32: Right-turn torque vectoring fine tuning. Driver: Ray Molina. Car: Epsilon.

5.5 Dynamic Torque Vectoring Results

With the performance results on the fixed skid pad, it is possible to calibrate the dynamic torque vectoring system in order to take into account a variety of possible turn radii and turn speeds. Based on the skid pad results for Epsilon, a dynamic torque vectoring range of 40-100% was chosen, meaning that the system was calibrated as per Eqn. 4 and Fig. 12 to provide

maximum torque at zero steering angle and full throttle displacement, but reduce the inside wheel torque during a turn to a minimum of 40% at maximum α and full throttle displacement. Due to the nature of the parallel throttle system, as per Fig. 12, this results in an effective minimum throttle output on the inside wheel under full load conditions of 50%, which corresponds well to the overall best performing setting during the static tests.

Phase 3 consisted of testing the chosen dynamic settings based on the Phase 2 results for both vehicles on the skid pad. Gamma, due to the control and time results, was selected for a 65-100% torque bias range, allowing for a medium between the lap time performance of the 50% setting and the stability of the 70% setting, while Epsilon was selected to maintain a 40-100% torque bias range.

The results for Gamma on the Skid pad for four different drivers, two novice (Adrian and Hieu), and two experienced (Jay and Drew) drivers is shown below in Fig. 33:

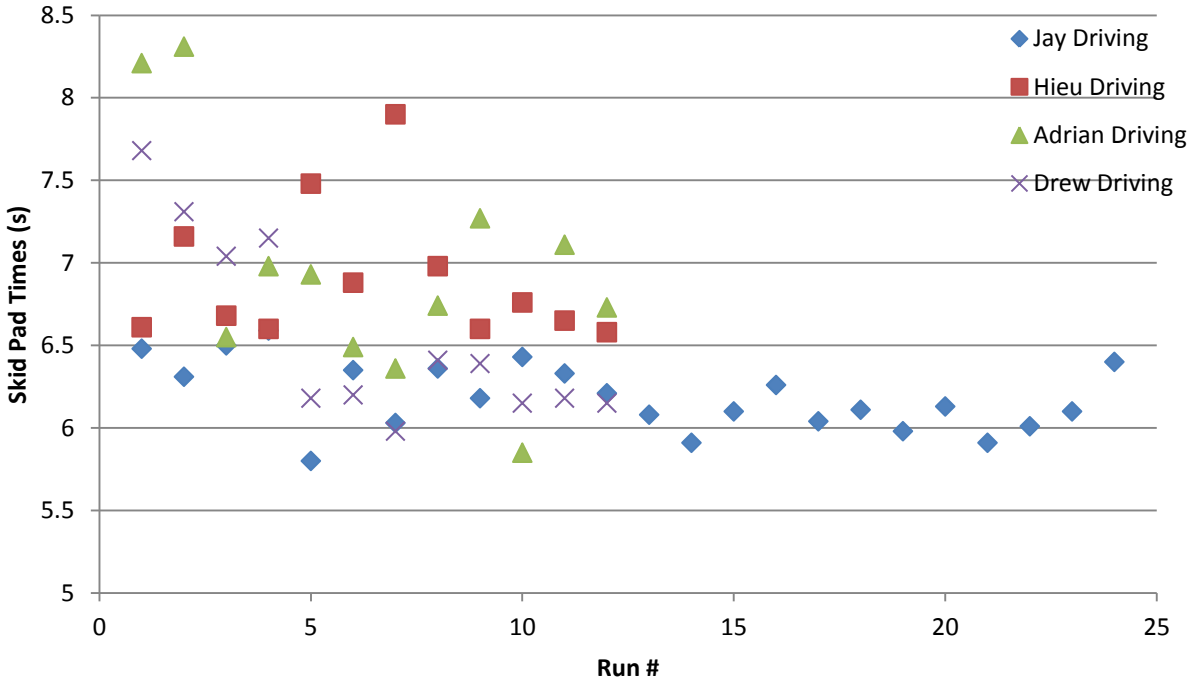

Figure 33: Gamma Phase 3 skid pad times. 65-100% torque bias range.

The same training as for the baseline had to occur for the Phase 3 testing; due to the fact that the drivers were used to a vehicle that had a constant inside torque bias and were changing to a vehicle that behaved similar to having a limited-slip differential for Phase 3. A comparison between the performance of Gamma's main driver for Phase 3, the baseline, and the Phase 2 settings is shown below in Fig. 34:

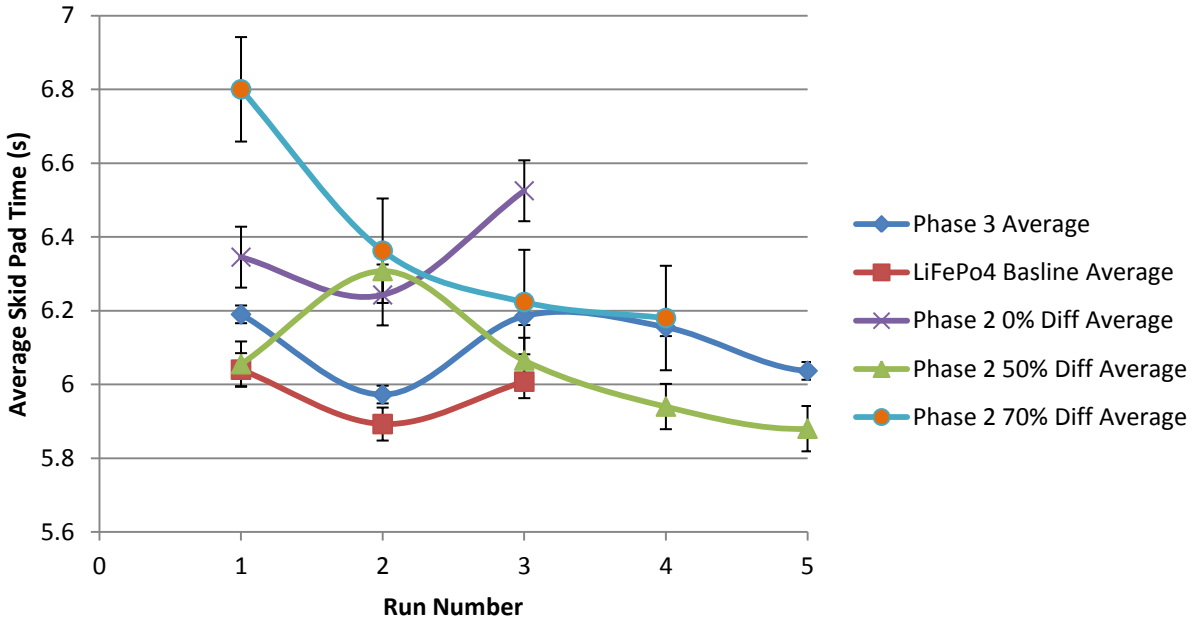

Figure 34: Phase 3 average skid pad times. Driver: Jay. Car: Gamma.

As Fig. 34 shows, the Phase 3 average times are on par with the 50% best times and are approaching the baseline results, showing an improvement over the 70% setting results. The largest impact, however, of the Phase 3 setting for Gamma is shown in Table 7.

Table 7: Gamma Phase 3 stability results.

	Number of Runs	Irrecoverable Failures	Percentage
Baseline (100%)	80	27	34%
Phase 2 0%	24	14	58%
Phase 2 50%	24	6	25%
Phase 2 70%	46	0	0%
Phase 3 (65-100%)	**28**	**0**	**0%**

Phase 3 shows a performance improvement over the 70% setting in terms of skid pad lap times as well as a stability improvement over the 50% setting. Driver feedback indicates a part of this is due to the nature of the dynamic VTS, as it allowed countersteer and correction techniques used by the drivers to adjust from a pure inside-to-outside torque deficit.

Figs. 35 and 36 shows the left- and right-hand turn results of Epsilon's Phase 3 setting compared to their 50% and baseline settings for both drivers. In both cases, the skid pad times are better than the baseline times, and driver feedback has indicated that controllability has improved, as well.

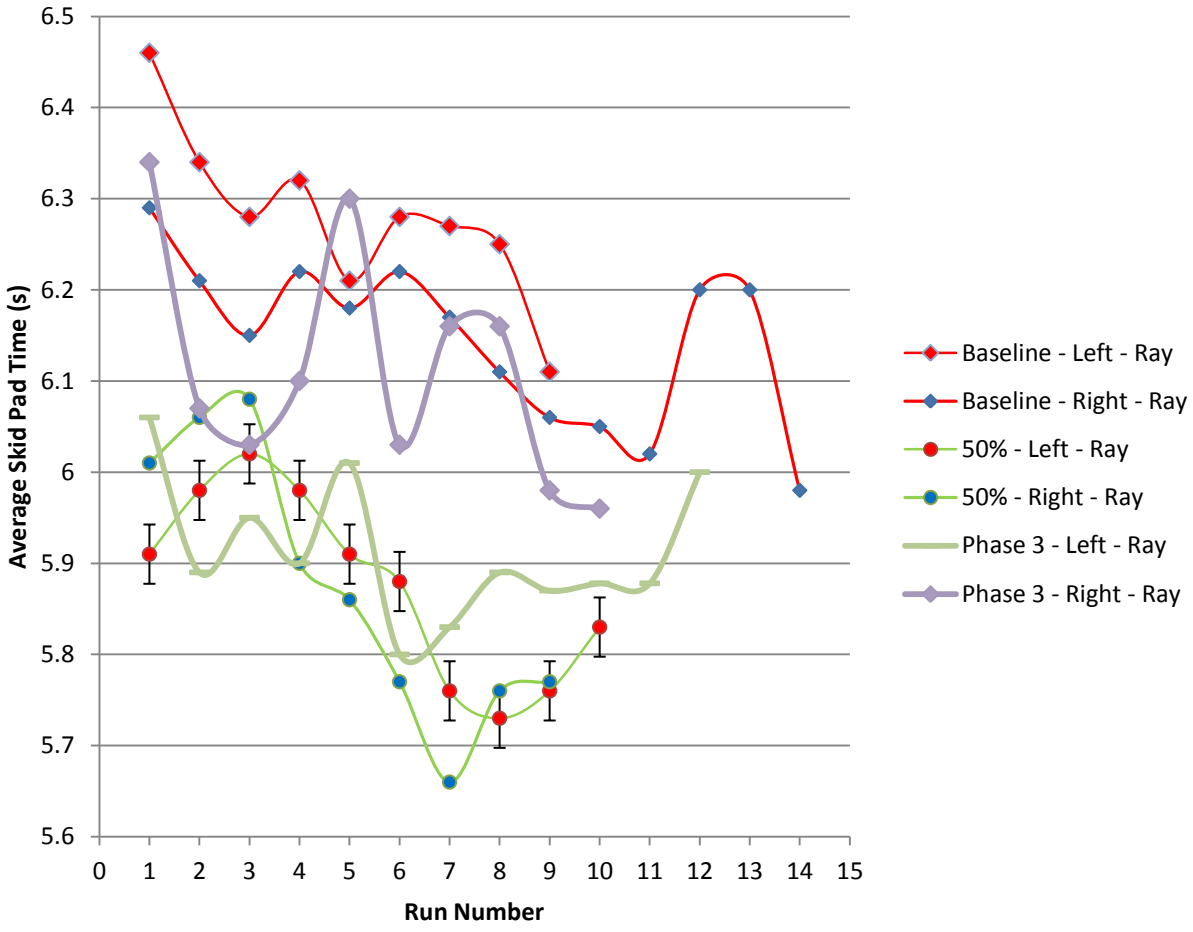

Figure 35: Phase 3 skid pad comparison. Driver: Ray Molina. Car: Epsilon.

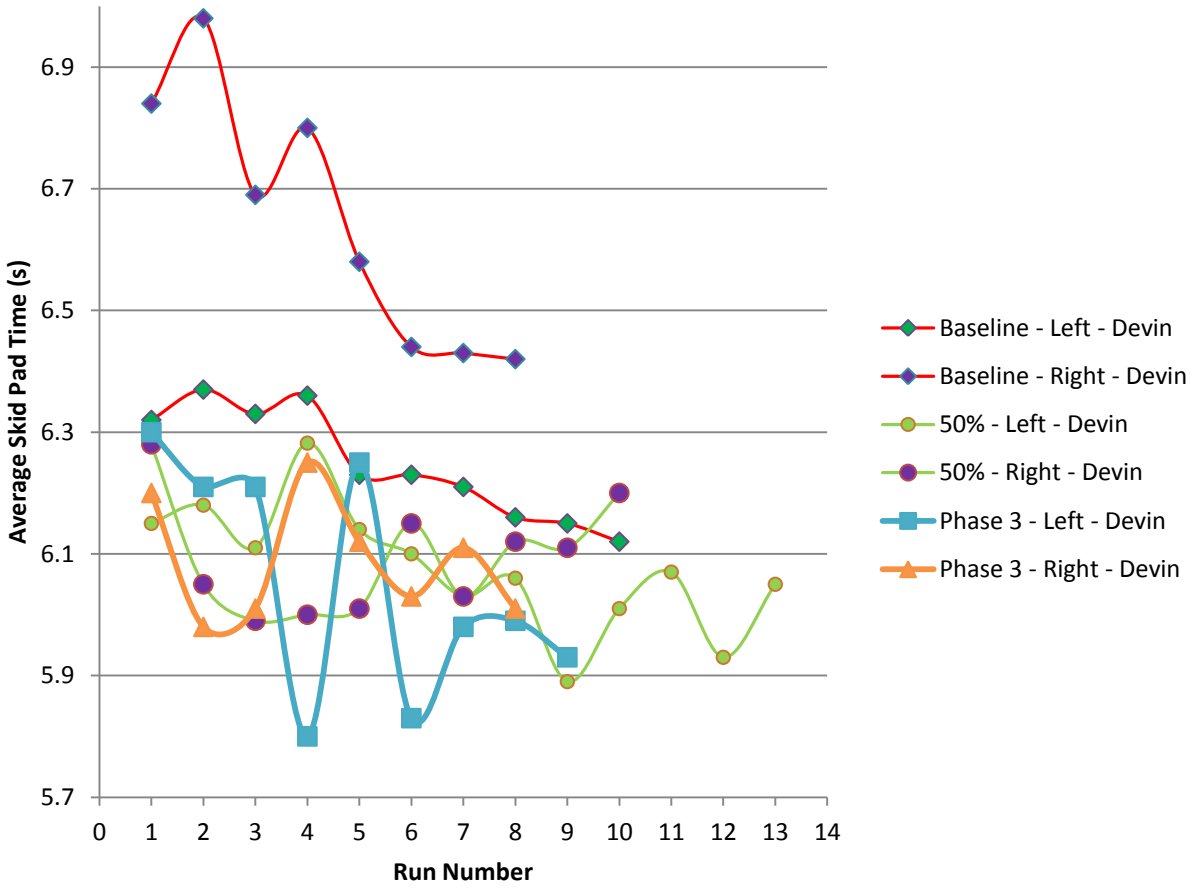

Figure 36: Phase 3 skid pad comparison. Driver: Devin Staal. Car: Epsilon.

An addition to Phase 3 was tested on the double-inverted figure four track described above, in order to assess the effectiveness of the system on an actual track involving multiple turns in different directions and of different radii and speeds. Three drivers were selected to run the course, with the overall result shown below in Fig. 37. The driver histogram on the DIFF shows that by taking the track for the first few times, driver times are still improving as the drivers continue to learn how fast the corners can be taken.

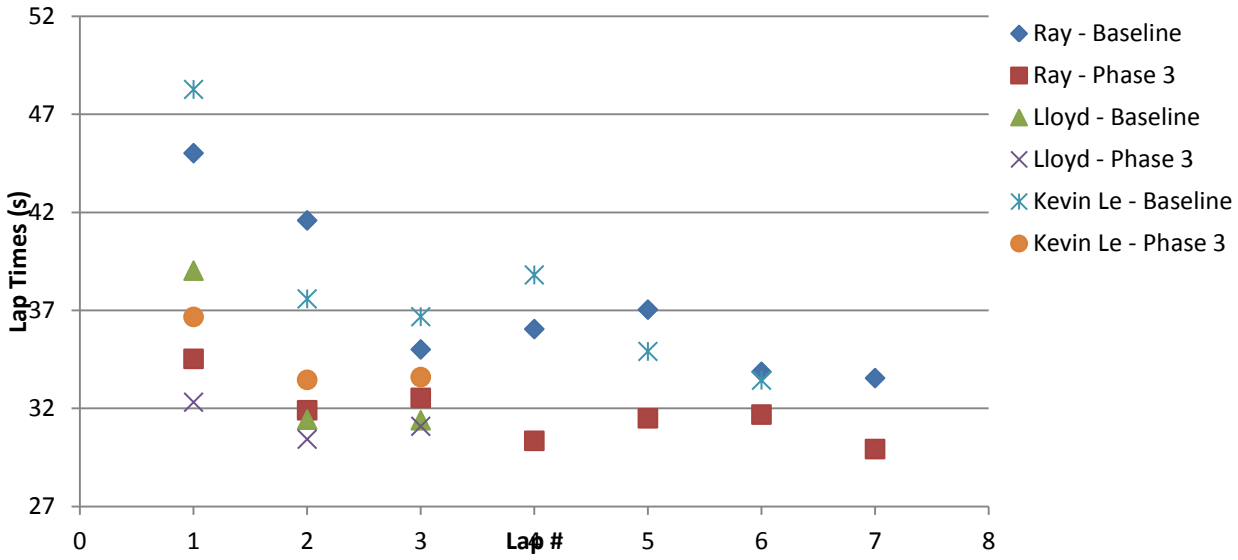

Figure 37: Lap times on the DIFF

Figs. 38-40 show a more detailed breakdown of the lap times on a per-driver basis, comparing the lap performances with and without the torque vectoring system.

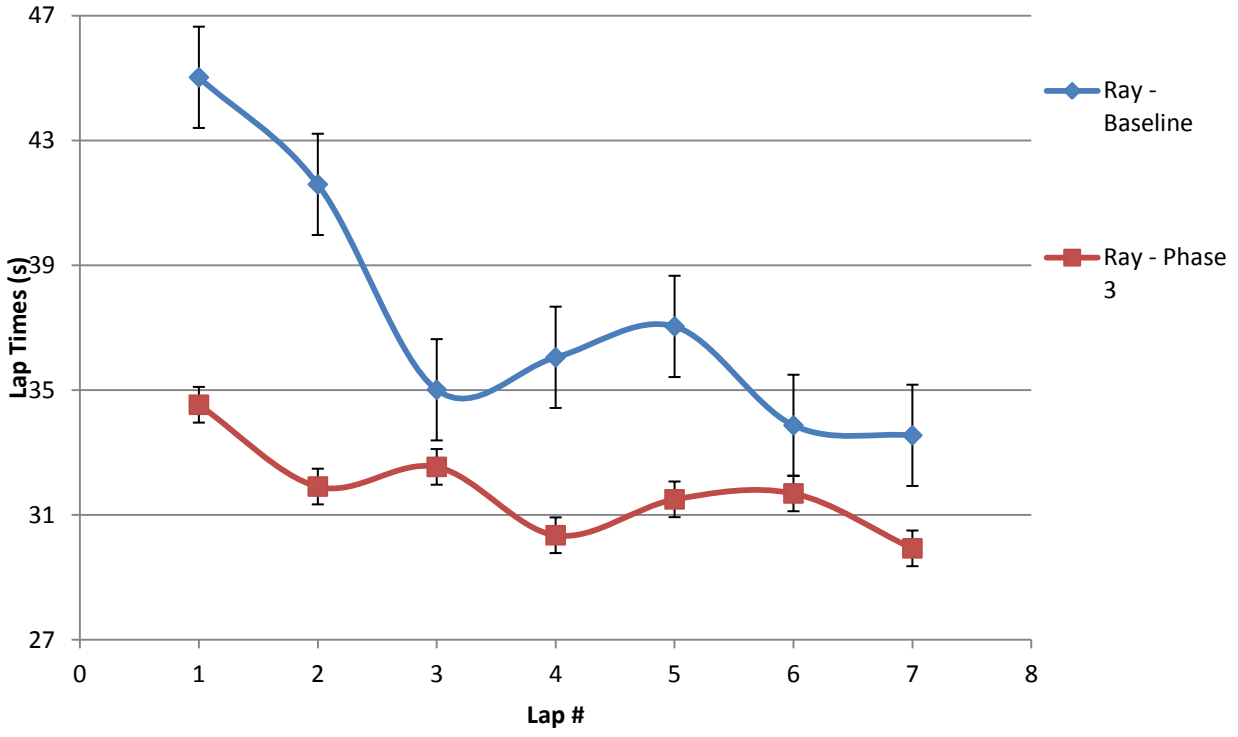

Figure 38: Lap times on the DIFF. Driver: Ray Molina. Car: Epsilon.

Lap times with the torque vectoring system were consistently and significantly faster than for the baseline, a trend that repeats in Figs. 39 and 40 for the other drivers, though the improvement margin varies from driver to driver, with Fig. 39 showing the data for an exceptional driver. Naturally, the potential for driver error is larger on the track due to the non-static nature of the velocity and turn radii; however, all drivers have noted that the vehicle handles better with the torque vectoring system active.

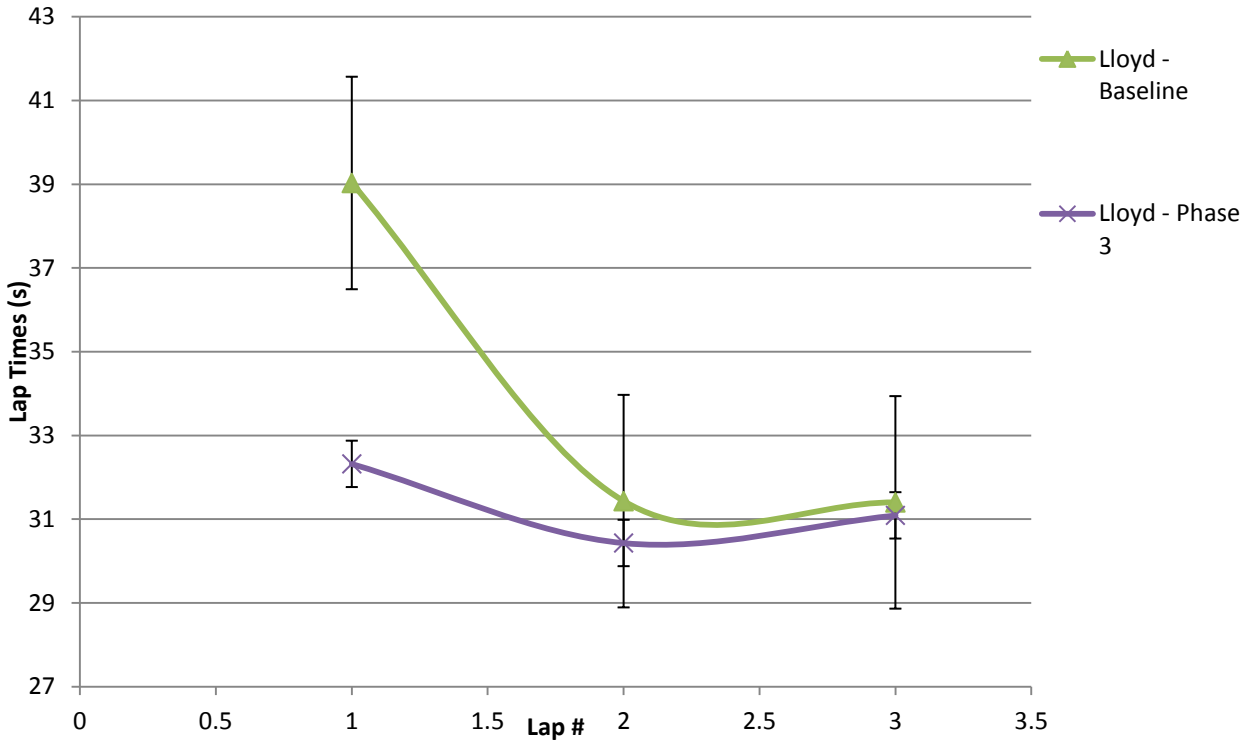

Figure 39: Lap times on the DIFF. Driver: Lloyd. Car: Epsilon.

Fig. 40 below shows a similar trend for the remaining driver, with a smaller margin of improvement from the baseline for the torque vectoring system, while Fig. 41 shows a comparison of the baseline results for all three drivers. Similarly, Fig. 42 displays the vectored times for all three drivers.

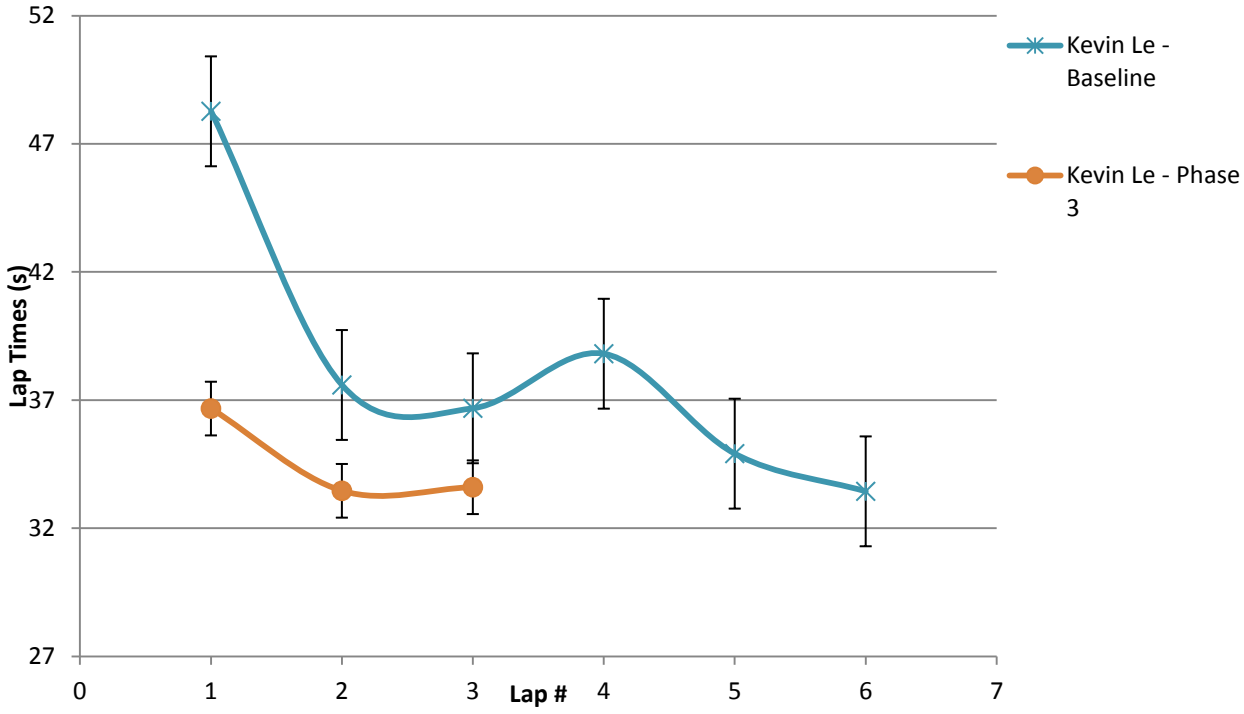

Figure 40: Lap times on the DIFF. Driver: Kevin Le. Car: Epsilon.

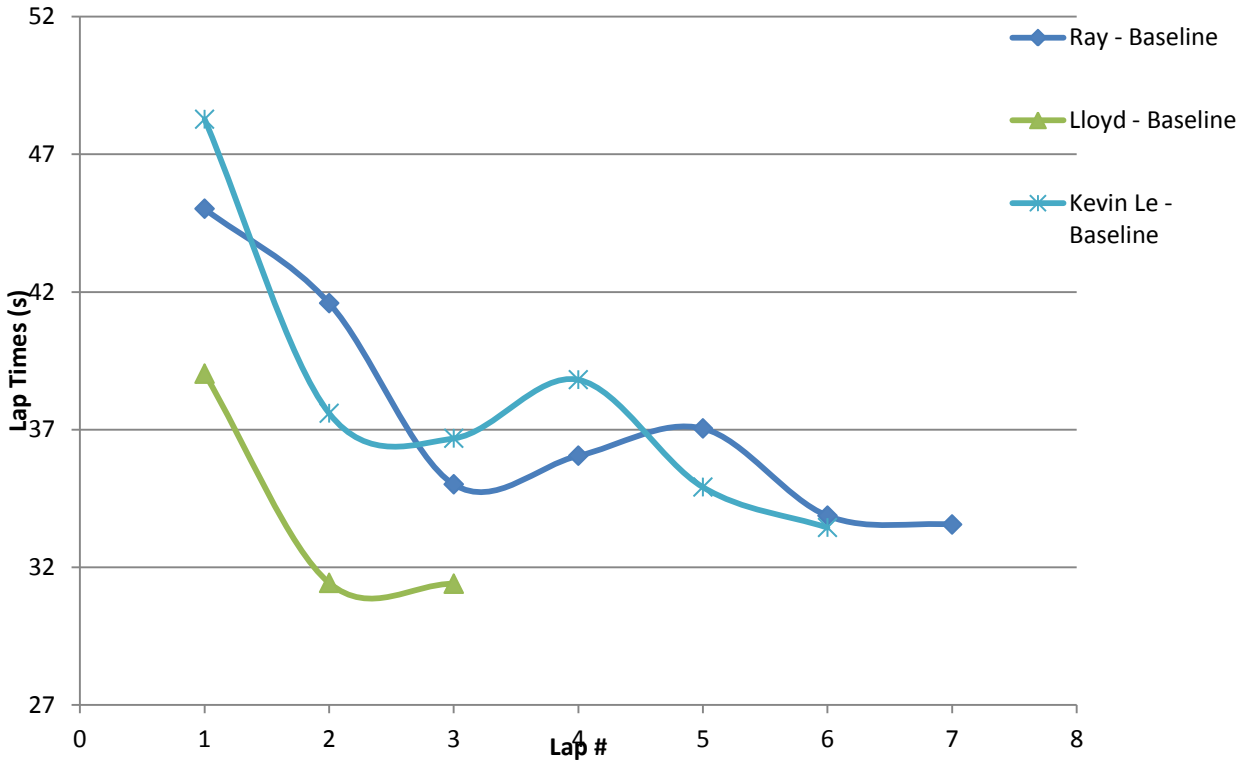

Figure 41: Baseline times on the DIFF for all drivers.

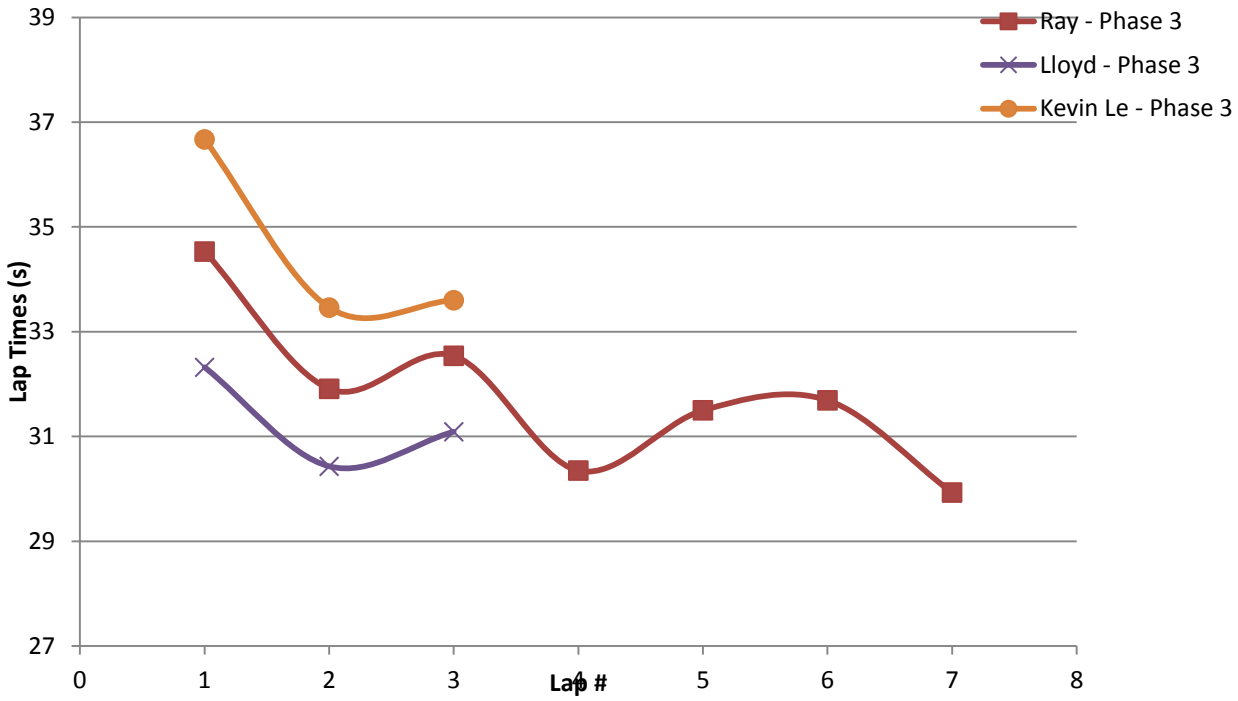

Figure 42: Phase 3 lap times on the DIFF for all drivers.

While the drivers have very distinct performances, in all but one case - who was an exceptional driver - the average baseline time to cover the DIFF track is 37s, while with the VTS active, the slowest lap time was under 37s. However, due to the length and nature of the DIFF track as well as the limited sample size, the error band is significantly larger than on the skid pad, making it less clear if the improvement in skid pad times is solely due to the VTS, or whether it is due to improvement in the driver's skill. It should be noted, though, that the largest sample of the primary driver indicates that while there is some fluctuation in the lap times, the torque-vectored times show much less variation amongst themselves and are outside of one standard deviation of the baseline times.

Similarly, it should be noted that due to the limited number of data sets taken from the DIFF course, baseline and vectored runs were alternated in order to mitigate driver learning hysteresis.

5.6 Overall Performance Comparison

Table 8 shows a summary of the stability results for Gamma; as Epsilon was, by nature, stable enough to not cause the driver to spin out as decisively. While for the heavier, oversteering Gamma, the majority of aborted runs were due to a total loss of control and spin-out, most aborted runs for the lighter, understeering Epsilon were caused by a recoverable failure, often causing the driver to retain control but necessitating a reset of the course for safety.

Table 8: Overall stability results for Gamma and Epsilon.

	Runs Gamma / Epsilon	Spin Outs Gamma / Epsilon	Percentage Gamma / Epsilon
Baseline	80 / 70	27 / 9	34% / 13#
Phase 2 70% / 75% TV	46 / 20	0 / 0	0% / 0%
Phase 2 50% TV	24 / 20	6 / 0	25% / 0%
Phase 2 0% / 10% TV	24 / 20	14 / 0	58% / 0%
Phase 3	28 / 36	0 / 0	0% / 0%

The Phase 3 results show the same stability for Gamma as the 70% vectored torque, which mitigates the natural oversteer of the vehicle. As Epsilon has not suffered the same kind of loss of control except for one driver, there is no similar statistic for the second car, though it may be telling that the one case where control issues where prevalent - with a highly inexperienced driver - the torque vectoring allowed him to complete a full set of laps that he had been unable to complete without.

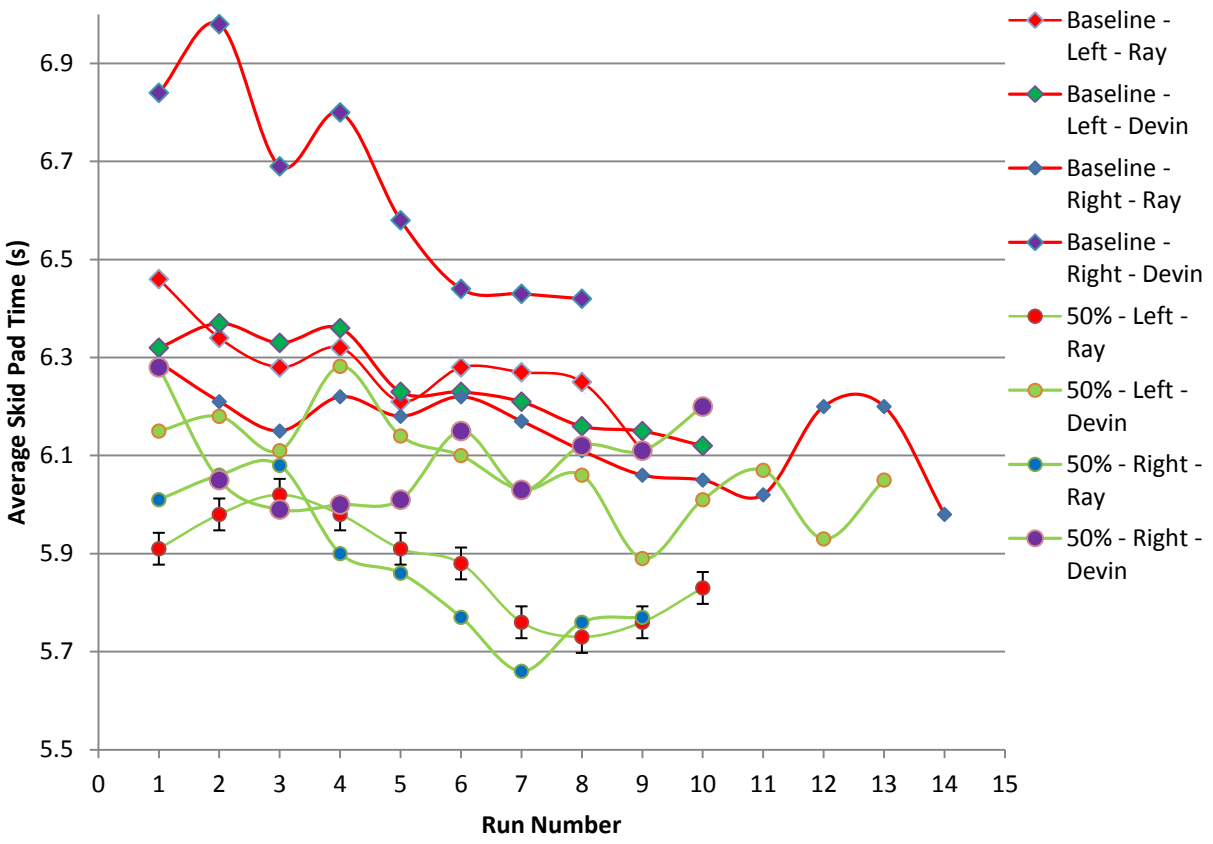

Figure 43: Test results for Epsilon's main drivers at neutral torque bias.

Fig. 43 shows a summary of major skid pad results for Epsilon for the two main drivers, while Fig. 44 shows the same results for Gamma for its sole main driver. While for Epsilon, the skid pad times with active VTS are consistently faster for both drivers, the improvement is not constant, and is dependent on the individual driver, as well.

Fig. 44 shows that in contrast to the results for Epsilon, the heavy, oversteering Gamma did not benefit as decisively from the torque vectoring; however, the torque control improved stability and reduced the fluctuations in skid pad times while maintaining the overall average performance of the vehicle in terms of lap times.

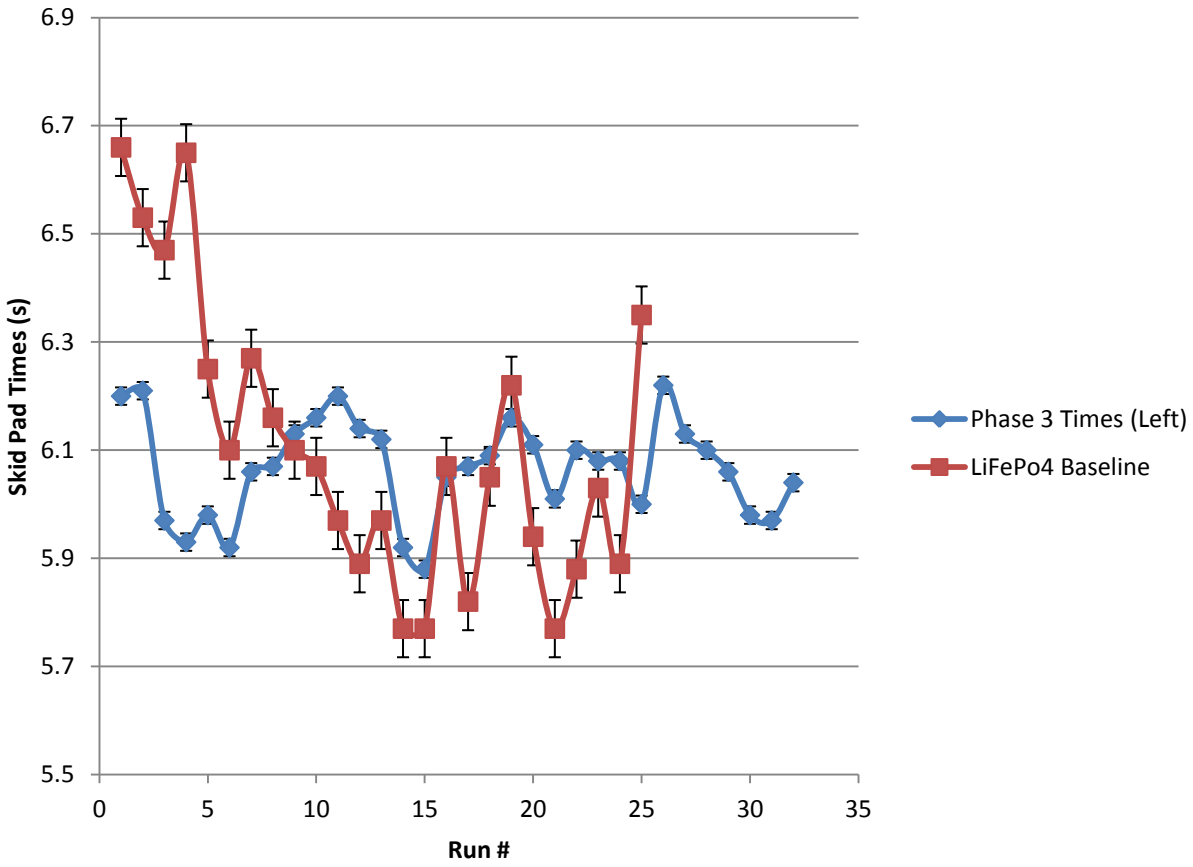

Figure 44: Test results for Gamma's main driver at a 67-100% dynamic TV setting.

6. Conclusions

6.1 Introduction

The objective of this research thesis was to investigate the effects of a vectored torque control drive system on the performance of a racing-type vehicle under high lateral accelerations. Two vehicles were compared: a heavy, innately oversteering car with a rear-heavy weight distribution and a large planform area, as well as a lighter, more compact, innately understeering car with a more even weight distribution. The effects of each vehicle were compared and assessed in order to draw a conclusion of the effectiveness of the vectored torque as well as possible effects of the vehicle characteristics on said effectiveness

A large number of skid pad experiments were conducted in order to measure the effects of various torque differentials between the inside and outside wheels during a high-speed turn at the traction limit in order to generate the two main metrics used in this theses: the maximum skid pad time - and therefore, the maximum lateral acceleration allowed by the car - as well as the stability in terms of handling and driving characteristics, quantified by the number of "spin-outs," or irrecoverable loss of control by the driver.

6.2 The Impact of Vectored Torque

While for Gamma, the torque vectoring did little to improve actual skid pad times, it did significantly improve the stability of the vehicle for both new and seasoned drivers; this is likely due to the weight of the car, as the net loss in power due to the torque bias is more significant on a heavy platform than on the lighter Epsilon. Conversely, on the lighter Epsilon, the torque vectoring did show a consistent improvement over the baseline measurements in most cases, while remaining on par with the baseline in the rest. When considering the innate stability of

both cars, driver feedback has yielded that despite the 30-70 front-to-back weight distribution on Gamma, the vehicle is highly oversteering, while the lighter Epsilon tends to be innately understeering.

Taking into account the skid pad results for both vehicles, as well as the stability metric, Gamma benefitted more in regards to handling and improved driving characteristics, which in turn yielded more reliable and better skid pad times despite the overall loss of net power. Similarly, Epsilon received a similar improvement in driving characteristics; however, the effect is much more distinct on Epsilon from a pure performance point of view and less so from a stability metric, and yielded a distinctly visible and measurable improvement in lap times despite the loss of net power.

However, both vehicles showed an improvement with the VTS active; though in the case of Gamma it was a stability-oriented benefit, while Epsilon yielded improved skid pad times. Both vehicles resulted in drivers noting afterwards that the addition of the VTS made the vehicle more stable and manageable during the skid pad and track runs. The more important conclusion that can be drawn from the data, however, is that even though the VTS was calibrated and the torque limits calculated by using solely using the basic chassis characteristics, it has shown an improvement in vehicle performance on both platforms. As the calculations for the weight transfer and resulting traction and torque limits are based only on the chassis parameters, the same calculations can be made for virtually any car under similar conditions.

The results may differ from vehicle to vehicle, as shown clearly by the different improvement margins of Epsilon and Gamma; however, in lieu of a mechanical differential, an electronic differential is necessary at the very least to reduce wheel drag. For vehicles that undergo high lateral acceleration conditions, a further addition like the VTS to the basic

electronic differential can further benefit the vehicle. Both Epsilon and Gamma were originally designed as competitive race cars in their size class; depending on the vehicle application, not all cars may see the same results. However, it can be extrapolated that improvement is possible regardless of the chassis, of up to 10%, in pure skid pad times and thus tolerable lateral acceleration before the onset of side-slip.

6.3 Recommendations for Future Work

More extensive testing should be conducted on a variety of vehicles with different driving characteristics. While it was found that Eqn.1 is useful to predict the theoretical optimal torque bias percentage, driver skill also plays a role in the resulting data. However, it was determined that for both vehicles, vectored torque was able to significantly alter the driving characteristics of the vehicle, capable of mitigating and, in some cases, eliminating oversteer or understeer. The benefit was less seen on the rear-heavy Gamma as, due to its weight and rear-wards weight distribution, the car tended to side-slip less for an experienced driver, and the effects that were seen were mostly impacting the stability metric as a good driver with control of the oversteer could post similar times with and without the torque vectoring.

Neither vehicle used for this research had a perfect 50-50 front-to-back weight distribution, and the effects of this system on both heavier and lighter vehicles, as well as those with a more even weight distribution should be considered for future work, as it is theorized that the more even the weight distribution - thus resulting in a more innately neutrally stable car that neither understeers nor oversteers - the less the benefit of the vectored torque. However, such a result would be dependent on the side-slip limit of the vehicle given by the inside-to-outside and front-to-back weight transfer that occurs during a turn as a function of turn radius and turn

velocity, as well as the traction afforded by the tyres under those conditions and whether the vehicle is capable of exceeding this limit on a regular basis.

Similarly, further testing needs to be conducted under actual live road driving conditions; as mentioned earlier, skid-pad testing only provides the base data for the calibration of the system. However, for any type of car, the actual behavior under live driving conditions differs from the static skid-pad conditions. Drivers rarely enter or exit turns at the optimal speeds just shy of inducing side-slip, and most tend to make minute adjustments during the turn. Other cases involve deliberately inducing and maintaining slide-slip in order to drift - something else that the VTS may be beneficial for. In all cases, though, the VTS is calibrated under static, ideal conditions at the edge of the vehicle's traction limit. While shown to be beneficial there, track testing has shown that even under less ideal circumstances, the VTS also benefits the vehicle and driver by compensating to the rapid adjustments made while driving.

6.4 Summary

This thesis has begun with the estimation of the weight transfer and subsequent resulting loss in traction budget for a vehicle undergoing a turn of a fixed radius at a set velocity and produced experimental data in an attempt to verify those calculations. Experiments were conducted with two vehicles of different driving characteristics and multiple different drivers on the skid pad as well as a custom track. In both cases, the vectored torque system benefitted the performance of the vehicle and driver in terms of controllability as well as lap time, an improvement that is visible across both vehicles independent of the driver.

The data and driver feedback have also shown that a VTS can affect and mitigate a vehicle's oversteer and understeer, thus affecting the natural driving characteristics of the vehicle, allowing it to be changed to optimize its performance and driver. Though the VTS used in this

thesis is a simple analog design that is vastly different from the digital DTC and flux-controlled systems currently under development for electronic differentials, it is more advanced than a basic DTC control scheme, taking into account several variables not present in most DTC schemes [2]-[4], most notably the throttle and steering position. While not as sophisticated as neural-network DTC systems, it has been shown to handle well at low and high speeds, as well as a range of different turn radii with significant performance benefits in a robust and simple system. The use of a torque and steering encoder allows for dynamic adjustment based on the current driving situation and allows a driver to directly control the torque differential by simply applying more or less throttle instantly during a turn, causing the system to adjust the torque differential appropriately in real time, combining the reaction time of a DTC scheme with the adaptability of an observer-oriented flux-controlled scheme.

More importantly, however, is that the data has shown the VTS to be beneficial with regards to the skid pad times - and thus, the overall side-slip limit of the vehicle - as well as controllability of the vehicle regardless of the driver or vehicle used for testing. The initial calculations for the VTS calibrations were made using nothing but the basic chassis characteristics; disregarding even the motor performance aside from the torque control curves. Despite this limited approach, the VTS has yielded significant benefits for both test vehicles, and the results can be further extended to any chassis with an applicable powertrain.

Performance improvements may vary from one platform to another, as shown clearly between Epsilon and Gamma, based on the overall vehicle weight and chassis parameters as well as available power. Gamma benefitted less in terms of direct skid pad lap time improvements than Epsilon due to the fact that the heavier chassis and higher traction limit caused the net power loss from vectored torque (due to powering down the inside wheel to match the traction

limit) to be more significant than on the lighter Epsilon, which had more excess power-to-weight. However, even despite the net power loss from the VTS, Gamma performed as well on the skid pad with the VTS as it did on its baseline runs, with improved stability.

Similarly, Epsilon showed a straight 10% improvement in skid pad times as well as track times on the DIFF with the VTS active, while stability results for Epsilon are as of yet unresolved due to lack of viable data. However, the improvement of both vehicles by the use of only basic parameters indicates that the same control scheme can be implemented on other vehicles and similar results can be expected within the given margins.

Bibliography

[1] F. J. Perez-Pinal, I. Cervantes, and A. Emadi, "Stability of an electric differential for traction applications," *IEEE Transportation Vehicle Technology*, vol. 58, no. 7, pp. 3224–3233, Sep. 2009.

[2] B. Tabbache, M.E.H. Benbouzid, A. Kheloui, "An adaptive electric differential for electric vehicles motion stabilization," *IEEE Transactions on Vehicular Technology,* 2011, *60,* 1, 104-110.

[3] A. Haddoun, M.E.H. Benbouzid, D. Diallo, "Modeling, analysis, and neural network control of an EV electronic differential," *IEEE Trans. Ind. Electron.*, vol. 55, no. 6, pp. 2286-2294, June 2008.

[4] N. Mutoh, Y. Hayano, H. Yahagi, K. Takita, "Electric braking control methods for electric vehicles with independently driven front and rear wheels," *IEEE Trans. Ind. Electron.*, vol. 54, no. 2, pp. 1168-1176, April 2007.

[5] J. Wang, Q. Wang, L. Jin, C. Song, "Independent wheel torque control of 4WD electric vehicle for differential drive assisted steering," *Mechatronics,* 2011, *21,* 1, 63-76.

[6] B.C. Besselink, "Computer controlled steering system for vehicles having two independently driven wheels," *Computers and Electronics in Agriculture,* 2003*,* 39, 209-226.

[7] Jang Bong-Choon, Yun Yeo-Heung, Lee Seong-Cheol, "Simulation of vehicle steering control through differential braking," *International Journal of Precision Engineering and Manufacturing*, 2009, 5(2). 26-34.

[8] A. Haddoun, F. Khoucha, M.E.H. Benbouzid, D. Diallo, "SDTC neural network traction control of an electric vehicle without differential gears," in *Proc. IEEE VPPC*, Arlington, TX, September 2007, pp. 259-266

[9] A. Haddoun, M.E.H. Benbouzid, D. Diallo, "A loss-minimization DTC scheme for EV induction motors," *IEEE Trans. Veh. Technol.,* vol. 56, no. 1, pp. 81-88, January 2007.

[10] F. Khoucha, S.M. Lagoun, K. Marouani, A. Kheloui, M.E.H. Benbouzid, "Hybrid cascaded H-Bridge multilevel-inverter induction-motor-drive direct torque control for automotive applications," *IEEE Trans. Ind. Electronic.,* vol. 57, no. 3, pp. 892-899, March 2010.

[11] I. Vincente, A. Endemano, X. Garin, M. Brown, "Comparative study of stabilising methods for adaptive speed sensorless full-order observers with stator resistance estimation," *IET Control Theory Applications*, vol. 4, no. 6, pp. 993-1004, June 2010

[12] J. Guzinski, H. Abu-Rub, M. Diguet, Z. Krzeminski, A. Lewicki, "Speed and load torque observer application in high-speed train electric drive," *IEEE Trans. Ind. Electron.*, vol. 57, no. 2, pp. 565-574, February 2010.

[13] L. Harnefors, M. Hinkkanen, "Complete stability of reduced-order and full-order observers for sensorless IM drives," *IEEE Trans. Ind. Electron.*, vol. 55, no. 3, pp. 1319-1329, March 2008.

[14] Hiromichi Nozaki, "Effect of differential steering assist on drift running performance," *SAE technical paper*, 2005-01-3472, 2005.

[15] S. Merkt, T. Gilbert, "Electronic Differential and Hybrid Powertrain Design for NCSU Formula Hybrid FH.2009," *North Carolina State University*, 2009.

[16] W. F. Milliken, D. L. Milliken, "Race Car Vehicle Dynamics," *Society of Automotive Engineers*, Warrendale Pa., 1995.

[17] F. Monti, "Hybrid and electric vehicles: powertrain architecture and sizing design," *Politecnico di Torino*, Torino, 2010.

[18] E. Hering, K.-H. Modler, "Grundwissen des Ingenieurs," Fachbuchverlag Leipzig, Leipzig, Germany, 2002.

[19] F. Nemry, G. Leduc, A. Munoz, " (F. Nemry 2009)," *European Commission Joint Research Centre - Institute for Prospective Technological Studies*, Luxembourg, 2009.

[20] A.F. Burke, C.B. Somuah, "Power Train Trade-Offs for Electric and Hybrid Vehicles," *Vehicular Technology Society IEEE*, paper no. 80CH1601-4, 1980.